LBL-34436

Glazing Materials for Solar and Architectural Applications

A final report of Task 10: Materials Research and Testing

September 1994

C.M. Lampert, Editor
Building Technologies Program
Energy and Environment Division
Lawrence Berkeley Laboratory
University of California
Berkeley, CA USA

INTERNATIONAL ENERGY AG
Solar Heating & Cooling Progra

DISCLAIMER

LBL-34436

Glazing Materials for Solar and Architectural Applications

Final Report

Dr. Carl M. Lampert, Editor
Building Technologies Program
Energy and Environment Division
Lawrence Berkeley Laboratory
University of California
1 Cyclotron Road
Berkeley, CA 94720 U.S.A.

Prepared for the International Energy Agency
Solar Heating and Cooling Program
Task 10—Solar Materials R&D
Subtask C—Glazing Materials

September 1994

This work was supported by the Assistant Secretary for Energy Efficiency and Renewable Energy, Office of Building Technologies, Building Systems and Materials Division of the U.S. Department of Energy under Contract No. DE-AC03-76SF00098.

TABLE OF CONTENTS

Participants in the Task 10 Glazing Materials Subtask

C. M. Lampert, Lawrence Berkeley Laboratory, Energy and Environment Division, University of California, 1 Cyclotron Rd. (MS 62-203), Berkeley, CA 94720 USA.

V.-V. Truong, University of Moncton, Faculty of Sciences, Department of Physics, Moncton, New Brunswick, E1A 3E9 Canada.

J. Nagai, Asahi Glass Co., Ltd., Advanced Glass R & D Center, 1150 Hazawa-cho, Kanagawa-ku, Yokohama 221, Japan.

M. G. Hutchins, Oxford Brookes University, School of Engineering, Oxford, OX3 0BP, UK.

F. Aleo, P. Carbonaro, A. Ferriolo, Conphoebus, Piano Diarci, Zona Industriale, 95030, Catania, Italy.

P. van Konynenburg*, formerly with Taliq Corporation, a wholly-owned subsidiary of Raychem Corporation, 1277 Reamwood Ave., Sunnyvale, CA, 94089-2234 *(now with Raychem Corporation, 300 Constitution Drive, Menlo Park, CA, 94025, USA.

S. Tanemura and K. Yoshimura, National Industrial Research Institute, 1 Hirate-cho, Kita-ku, Nagoya, 462, Japan.

W. J. Platzer, V. Wittwer, M. Kohl, Fraunhofer Institute for Solar Energy Systems, Oltmannstrasse 22, D-7800, Freiburg, Germany.

U. Frei, School of Engineering, Solar Energy Lab. (ITR), CH-8640, Rappererwil, Switzerland.

K. G. T. Hollands., University of Waterloo, Department of Mechanical Engineering, Waterloo, Ontario, N2L 3G1, Canada.

S. A. Svendsen, Thermal Insulation Lab., Technical University of Denmark, Build. 118, DK 2800, Lyngby, Denmark.

B. Karlsson, Vattenfall, Swedish State Power Board, Ålvkarlby Lab., Ålvkarlby, S-810 71, Sweden.

J. Klems, Lawrence Berkeley Laboratory, Energy and Environment Division, University of California, 1 Cyclotron Rd. (MS 90-3111), Berkeley, CA 94720 USA.

ABSTRACT

This report summarizes five collaborative research projects on glazings performed by participants in Subtask C of IEA Solar Heating and Cooling Programme (SHC) Task 10, Materials Research and Testing. The projects include materials characterization, optical and thermal measurements, and durability testing of several types of new glazings. Three studies were completed on electrochromic and dispersed liquid crystals for smart windows, and two were completed for low-E coatings and transparent insulation materials for more conventional window and wall applications. In the area of optical switching materials for smart windows, the group developed more uniform characterization parameters that are useful to determine lifetime and performance of electrochromics. The detailed optical properties of an Asahi (Japan) prototype electrochromic window were measured in several laboratories. A one square meter array of prototype devices was tested outdoors and demonstrated significant cooling savings compared to tinted static glazing. Three dispersed liquid crystal window devices from Taliq (USA) were evaluated. In the off state, these liquid crystal windows scatter light greatly. When a voltage of about 100 V ac is applied, these windows become transparent. Undyed devices reduce total visible light transmittance by only .25 when switched, but this can be increased to .50 with the use of dyed liquid crystals. A wide range of solar-optical and emittance measurements were made on low-E coated glass and plastic. Samples of pyrolytic tin oxide from Ford glass (USA) and multilayer metal-dielectric coatings from Interpane (Germany) and Southwall (USA) were evaluated. In addition to optical characterization, the samples were exposure-tested in Switzerland. The thermal and optical properties of two different types of transparent insulation materials were measured. Samples of the polycarbonate honeycomb (supplied by Arel in Israel) and monolithic aerogel (supplied by Airglass in Sweden) were evaluated. Discrepancies in the round robin thermal measurements for the honeycomb material pointed out some measurement problems due to different equipment and procedures used. Overall, these glazing studies were successful in improving the understanding and use of advanced glazings. Follow-on work on most of these glazings will be continued in the new IEA SHC Task 18, Advanced Glazing Materials.

EXECUTIVE SUMMARY

This report summarizes the activities of the glazings group (Subtask C) for IEA Solar Heating and Cooling Programme (SHC) Task 10, Solar Heating and Cooling Materials Research and Testing. This group comprised researchers from nine countries. The studies carried out by the participating researchers chiefly involved the measurement of properties of new types of glazing materials, including switchable glazings, low-E coatings, and transparent insulation materials, the development of test and characterization methods, and physical testing of glazings in round-robin measurements. Most of the work reported here was carried out between 1988 and 1990. A summary of the chapters follows.

I. Overview of Optical Switching Technology

Large-area optical switching devices have an exciting future in glazing applications. By using various technologies, it is possible to change the optical density, energy transmission, and reflection properties of a glazing according to occupant and building needs. These glazings can serve as dynamic energy regulators rather than as static, fixed-property building elements. Electrochromic and dispersed liquid crystal windows are some of the best switchable technologies. In the Task 10 work, IEA SHC researchers developed much-needed characterization methods for both types of devices. Prototype electrochromic windows from Asahi Glass in Japan and dispersed liquid crystal glazings made by Taliq (Raychem) in the USA were tested as characterized.

II. Characterization Parameters and Test Methods for Electrochromic Devices in Glazing Applications

This chapter addresses the issues of characterization and testing of electrochromic devices. Currently there are no standards for these devices. As these devices become important for glazings, one must seriously look at characterization parameters and test methods for each parameter to see if they are appropriate or proper. It is the goal of this work to better standardize the parameters reported in the literature. A recommended method is proposed for each measurement parameter, and some new parameters are introduced. Included in this study are information and recommendations from several researchers and manufacturers of electrochromic devices. The parameters covered in this work are categorized into three major areas: optical properties, electrical properties, and efficiency measurements. Optical properties include solar and photopic transmittance, reflectance, and absorptance; optical density; and chromaticity coordinates. For electrical measurements, injected charge, impedance measurements, potential type, voltammetry, switching chronopotentiometry, point-of-zero-zeta-potential, and cycle energy and power are discussed. In the section on efficiency and response, the properties of coloration efficiency, response time, and memory are detailed. It was concluded that electrochromic glazings are not currently well enough characterized to accurately compare each glazing on a one-to-one basis. The authors have tried to standardize some of the more common measurements and added some proposed parameters, such as spectral and integrated coloration efficiency. Many of these parameters need to be developed further and brought to the attention of the national and international standards committees.

III. Measurement of the Asahi Prototype Electrochromic Window

This chapter summarizes work on the testing of the Asahi prototype electrochromic window (10 cm x10 cm). This window is the most commercialized of the electrochromic glazings. Several larger panes (30 cm x 30 cm) have been installed in Japan. In this study, the optical transmittance properties, both specular and integrated, were investigated under various conditions. Integrated visible transmittance changed from 0.78 to 0.20 when a voltage of –2.0 V was applied across the device. The transmittance–voltage dependency was determined for these devices. Memory and coloration rate were measured, and the chromaticity coordinates were determined. Additional characterization was performed on the MoWiTT (otdoor thermal test facility) using a matrix window assembly consisting of nine 30-cm x 30-cm windows. From this study it was concluded that the Asahi electrochromic window had very good light and energy control properties. It did not have memory, so power needed to be applied continuously. In the MoWiTT measurements it was found that, if the window transmittance is dynamically controlled to give constant interior illumination, a substantial amount of overheating of the workspace can be reduced. Even though the electrochromic glazing was absorptive in nature, it did substantially reduce heat flow through the window and thus reduces air conditioning loads. This technology is very promising for the next generation of windows.

IV. Optical Characterization of the Taliq Liquid Crystal Window

This chapter covers measurements on the Taliq type of phase-dispersed liquid crystal optical switching device (PDLC). Two categories of liquid crystal devices were studied, a conventional device and one containing a dyed liquid crystal that gave enhanced visible switching. Participants made measurements of its optical transmittance in both the normal and hemispherical modes, including both integrated and spectral measurements over the solar spectrum. Also, angular scattering measurements were performed. In conclusion, it was found that the typical PDLC device has very broad switching, but its net change in hemispherical transmittance was only about 25% over the solar and visible spectrum when 100 V ac is applied since much of the switching effect produces forward scattering. The dyed liquid crystals, however, showed much improved visible control of 50% change. These devices appear to be best suited for privacy and skylight applications.

V. Durability Testing of Low-E coatings

The measurement of normal and hemispherical optical and infrared emittances of commercialized low-E coatings (available at the time of the measurement) is the focus of this chapter. The study also included exposure testing of low-E coatings. Several coating types were tested including pyrolytic tin oxide from Ford Glass and dielectric/metal/dielectric (D/M/D) coatings from Southwall and Interpane. Sample solar and photopic (visible) transmission properties were as follows: Interpane, $T_{s,total} = 0.555$ and $T_{p,total} = 0.820$; Ford, $T_{s,total} = 0.753$ and $T_{p,total} = 0.834$; Southwall, $T_{s,total} = 0.695$ and $T_{p,total} = 0.855$. These samples were exposure tested (unprotected) at the Swiss Interkantonales Technikum Rapperswil test center. The results showed that the Southwall and Interpane D/M/D coatings were totally destroyed by exposure and the Ford coating was unchanged. For the D/M/D coating, these results were expected because of the inherent fragility of the materials used in the coatings. This confirmed that these types of D/M/D coatings can not be exposed to normal weathering without protective coatings.

VI. Interlaboratory Testing of Transparent Insulation Materials

Testing of commercial transparent insulation materials and glazings is reviewed in this chapter. Measurements of both thermal properties as well as angular and hemispherical optical properties were made. Two types of materials were investigated: a honeycomb polycarbonate made by Arel in Israel and an aerogel made by Airglass in Sweden. These samples were tested in a round-robin test procedure to verify each laboratory's test equipment and general accuracy. Sample results for the honeycomb (5 cm) were as follows: $T_{s,normal}$ = 0.93–0.95, $T_{s,diffuse}$ = 0.84, and U = 1.38–1.77 W/m^{2}K. Measurements for the Aerogel were as follows: $T_{s,normal}$ = 0.61–0.75, $T_{s,diffuse}$ = 0.53–0.60, and U = 0.99–1.07 W/m^{2}K. The range in values indicates the variation in measurements from different laboratories. It was found that some of the thermal test equipment in different laboratories gave significantly different results. Some common measurement problems were uncovered, such as edge conduction along highly insulating windows (e.g., aerogels). This study helped some of the participants improve their thermal measurement procedures.

I. OVERVIEW OF OPTICAL SWITCHING TECHNOLOGY

A. Introduction

Optical switching technology has a very natural place in future glazings. It is probably one of the most exciting areas in glazing technology and has the potential to change the concept of a glazing from that of a fixed element to that of a dynamic one (Lampert, 1984; Selkowitz and Lampert, 1990). All large-area switching processes are classified as "chromogenic" (Lampert and Granqvist, 1990). A glazing made of a chromogenic material can be used to control the flow of light and heat into and out of a window according to an energy management scheme. Optical switching devices can also regulate daylighting.

The basic property of an optical switching material or smart window is that it shows a large change in optical properties upon a change in either light intensity, spectral composition, heat, electrical field, or injected charge. This optical change results in a transformation from a highly transmitting state to a partly reflecting or absorbing state, over the visible or solar spectrum. The physical phenomena of interest for optical switching processes can be classified into one of two categories: discrete mass movement or collective physical movement. Discrete mass movement includes ion and localized electron motion as seen in photorefractive, photochromic, electrochromic, and thermochromic materials. Collective physical movement includes dispersed and homogeneous liquid crystals, suspended particles, deformable membranes, and adjustable diffraction gratings. The two most promising materials are electrochromic and phase dispersed liquid crystal (PDLC) devices. In this subtask, the properties of prototype examples from each of these groups were studied.

Some of the most significant issues are the cost of these devices and the trade-off between cost, lifetime, and benefit. Potential electrochromic window cost has been estimated to range from $100 to $1000 U.S. per square meter ($10–100 U.S. per square foot) . Currently, PDLC windows sell for about $1000 U.S. per square meter, with a future price reduction of possibly 30–50%. Research on these devices is aimed at long-life devices with durability similar to that of regular coated windows. It is expected that costs will decline with new materials, such as cheaper transparent conductors, and simplified production techniques.

Electrochromic windows are a very popular area of research; over the last ten years about 200 U.S. and international patents have been granted per year. Japan leads in patents granted by about 4:1 over the rest of the world. Electrochromism is exhibited by several inorganic and organic compounds (including some polymers). Electrochromism is of current research interest because of its application to optical switching windows and mirrors for buildings and vehicles and to large-area electronic information display devices. The major advantages of electrochromic materials are that they only require power during switching, have a long-term memory (12–48 h), require small voltage to switch (1–5 V dc), are specular in all conditions, and have the potential for large-area application. Electrochromic materials change their optical properties because of the action of an electric field and can be changed back to the original state by a field reversal.

There are two major categories of electrochromic materials: transition metal oxides, including intercalated compounds, and organic compounds. The electrochromic effect occurs in inorganic compounds by dual injection or by ejection of ions (M) and electrons (e^-). Materials can color cathodically or anodically. The inorganic materials that have gained the most research interest are NiO films and amorphous (a) and crystalline WO_3, MoO_3, and IrO_x. These compounds, among other transition metal oxides, are the subject of a few research reviews (Fanghan and Crandall, 1980; Dautremont-Smith,1982; Lampert, 1984; Oi, 1986; Donnadieu, 1989; Lampert and Granqvist, 1990). A typical reaction for a cathodic coloring material is:

$$WO_3 \text{ (transparent)} + yLi^+ + ye^- <-> Li_yWO_3 \text{ (blue)}$$

A typical anodic reaction is:

$$Li_xNi_{1-x}O \text{ (transparent)} <-> Ni_{1-x}O \text{ (bronze)} + xLi + xe^-$$

An electrochromic device must use an ion-containing material (electrolyte) in proximity to the electrochromic layer as well as transparent layers for setting up a distributed electric field. Devices are designed in such a way that they shuttle ions into and out of the electrochromic layer with applied potential. A solid-state window device can be fabricated from five (or fewer) layers consisting of two transparent conductors, an electrolyte or ion conductor, a counter electrode, and an electrochromic layer.

Electrochromic devices are composed of a variety of materials and device structures. There are five common structures ranging from three to five layers, depicted in Fig. 1. The elements of an electrochromic device are the electrochromic (EC) layer, ion conductor (IC), ion storage layer (IS), and transparent electronic conductor (TC). The ion storage layer is typically referred to as the counter-electrode. Another design uses an electrolyte (EL) (polymeric, organic, or inorganic) as a combined ion conductor and storage medium. Yet another design consists of organic electrochromic components mixed in the electrolyte. The five-layer designs are probably the most useful for glazing applications. Two five-layer designs are shown, one with a complementary electrochromic layer, another with an ion storage layer.

Characterization parameters are basic parameters used to evaluate or measure the property of a material or device. The parameter might measure an optical, electrical, or thermal property. More complex parameters might measure efficiency or some type of performance characteristic. The measured parameters may help improve or better evaluate the perfomance of electrochromic devices. Much international research is directed at the development of better component materials with high cycle lifetimes and short response times.

The current activity on electrochromic windows is largely for automotive applications, such as mirrors and sun roofs, and consumer items, namely sunglasses. These are ideal entry markets because of the smaller size and shorter lifetime required of the device, though the greatest potential market is still architectural windows. Many companies have their long-term goal directed at this market.

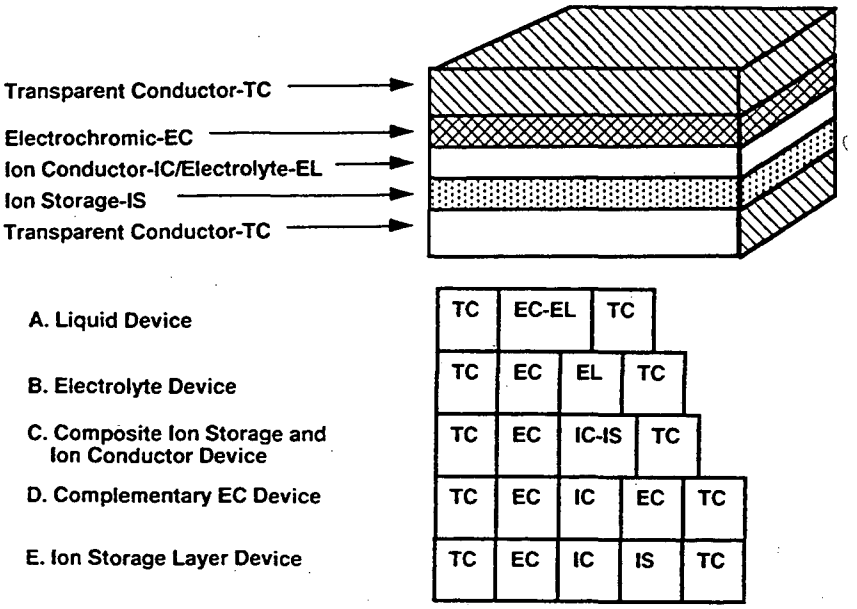

Fig. 1. Schematic cross-section and table of typical electrochromic device structures.

B. References

Dautremont-Smith, W. C., "Transition metal oxide electrochromic materials and displays: A review," Displays 4-3(1982)67.

Donnadieu, A., "Electrochromic materials," Mat. Sci. and Engin., B3(1989)185-195.

Faughan B. W. and Crandall, R. S., "Electrochromic displays based on WO_3" in Display Devices, (Pankove, J.I. edit.), Springer-Verlag, Berlin, Germany (1980).

Lampert, C. M., "Electrochromic materials and devices for energy efficient windows," Solar Energy Materials 11(1984)1.

Lampert, C. M. and Granqvist, C. G., edits., Large-area Chromogenics: Materials and devices for transmittance control, Optical Engineering Press- SPIE, Bellingham, WA, (1990).

Oi, T.,"Electrochromic materials," Ann. Rev. Mat. Sci. 16(1986)185.

II. CHARACTERIZATION PARAMETERS AND TEST METHODS FOR ELECTROCHROMIC DEVICES IN GLAZING APPLICATIONS:

C. M. Lampert, V.-V. Truong, J. Nagai, and M. G. Hutchins

Over the past few years, electrochromic devices for large-area applications have become important for glazing window applications (Lampert and Granqvist, 1990). Many of the characterization techniques for these devices are based on small-area information display devices or small-area mirror devices and not with a large-area transparent window in mind. Furthermore, many parameters measured on information displays are monochromatic, double pass in the reflectance or absorptance mode. Some parameters important to the glazing and glass industry are not measured currently. This study evaluates each parameter used to characterize an electrochromic device. It is analyzed in terms of appropriateness and of adequacy for a window application. This study will help guide researchers to a common set of characterization parameters, even if it is a minimal set. Currently, it is very difficult to evaluate different researchers' work because each determines the same parameter differently. One complication is that electrochromic devices are different and have different structures; they can consist of organic, inorganic, or mixed media. Very complex chemical and electrochemical reactions can occur in these devices.

It is not the purpose of this study to separate device designs or materials by different test methods. That is the subject of another in-depth study of specific designs and materials involving physical and chemical models. The purpose here is to present general methods, parameters, and guidelines. Some subjects may require further development for use with electrochromic devices. Some of these issues will be taken up in IEA Solar Heating and Cooling Task 18 (Glazings). Issues concerning stability, durability, and life testing are the subjects of two companion reports (Lampert, 1990, Czanderna and Lampert, 1990). A full version of the following study is available (Lampert et al, 1991).

A. Optical Properties

1. Solar and Photopic Transmittance, Reflectance and Absorptance

The majority of electrochromic materials are specular in nature, but sometimes hemispherical data are taken. Generally, a dual-beam spectrophotometer is used to make the measurements, with the wavelength range corresponding to the optical region of interest. Early work with display devices usually reported monochromatic or average (flat weighted) visible data. Monochromatic data are usually reported at the peak absorption wavelength. This is useful for time rate or voltage variation studies if the characteristics of the device are stable. However, the data can be misunderstood if the peak absorption shifts or changes with voltage, cycling, or time. In monochromatic cyclic studies, it is not clear if a real change in optical density was seen or the absorption peak shifted.

It is important to spectrally weight the optical properties of electrochromic devices for their intended application. In solar energy applications, solar weighted transmittance (T_S), reflectance (R_S), and absorptance (A_S) values are used. The standard used for the solar spectrum weighting

at Air Mass 1.5, is ASTM Standard E 891. For many applications the human response to the glazing is important. The daytime human eye response is known as the photopic response (Simon, 1974). The photopic or luminous (visible) response is in the 0.39-0.77 nm region. The photopic weighted transmittance (T_p), reflectance (R_p), and absorptance (A_p) values should be used to characterize electrochromic devices.

2. Optical Density

Optical density is a parameter used in optics and has been used to characterize electrochromic display devices. Optical density will be included since it is used to calculate coloration efficiency. It is used incorrectly in many papers in the literature. For example, the device changed in optical density of 1.0. Unfortunately, the reader would need a base value to judge the true transmittance change. If optical density is used, the base optical density must also be stated. It is more descriptive to use transmittance values or absorptance and should be given along with optical density. The change in optical density ($\Delta OD(\lambda)$) is used to determine coloration efficiency, discussed in Section C.1.

3. Shading Coefficient

The Shading Coefficient (SC) is a common term used by the glass industry to describe solar heat gain by glazings. The shading coefficient has been measured for a variety of fixed property glazings. The SC is a ratio of the Solar Heat Gain of the sample glazing (SHG_s) to the Solar Heat Gain of clear float glass (SHG_g), with a thickness of 3.175 mm (0.125 inch). Both glazings are tested under the same conditions. Since clear float glass has $T_s = 0.86$, $R_s = 0.08$, and $A_s = 0.06$, it is possible for a sample to have a higher SC than 1.0.

The shading coefficient has not been defined for switchable material with variable shading properties. The shading coefficient for a switchable film could be bounded by the extreme states of coloration, the bleached and maximum colored condition. In actual operation, the SC would be somewhere between these values depending on the operating conditions of the window. Standards for the measurement of SC for electrochromic windows are expected to be developed in the future. The concept of a variable shading coefficient has been applied to window energy modeling of switchable glazings (Reilly et al, 1991).

4. Measurement of Color—the Chromaticity Coordinates (CIE)

For electrochromic windows it is very important to be able to scientifically specify the colors of a window. The most common technique used by manufacturers to specify the color for a wide range of products is with the CIE (Commission Internationale de l'Eclairage) chromaticity coordinates. Chromaticity coordinates can be derived from spectrophotometry. Spectrophotometry depends only on measurements of the wavelength of light and measurements of transmittance, absorptance, or reflectance, all of which can be determined with accuracy. These coordinates provide a fundamental basis for a description of color. Color is specified by 3 non-physical primaries, denoted by X, Y, and Z. These can be derived from the red, green, and blue physical primaries (Murdoch, 1985, MacAdam, 1985). The corresponding spectral tristimulus values are denoted by x, y, and z. Only two of the values are needed to specify color

(normally x and y), as the third one can always be derived from the other two. Chromaticity can be conveniently represented by plotting the trichromatic coefficients, x and y, on a flat map. Two standard CIE systems are commonly used, CIE (1931) for 1–4° observer field-of-view angles and CIE (1964) for greater than 4° observer angles. The current CIE recommendation is to use Illuminant A or Illuminant D_{65} (close to a 6000 K blackbody) for the evaluation of colored objects (Murdoch, 1985).

If two materials have identical tristimulus values, they constitute a color match under the conditions for which the tristimulus values were determined. However, tristimulus values do not indicate in a readily comprehensible manner the nature of the color difference. It is then apparent that two colors can have the same chromaticity; the difference between them is a difference of a luminance factor. This relationship is not immediately evident from the tristimulus values. Two other factors are also used to specify an object color, they are the Dominant Wavelength and the Excitation Purity. The Dominant Wavelength (D_λ) is defined as the wavelength of radiant energy that, when combined with the radiant energy of a reference standard, matches the color of the light reflected or transmitted from the window. Excitation Purity (E_p) is defined as the ratio of the object and source on a line drawn to D_λ on the boundary of the diagram. The source is always 0% purity and the boundary is 100% purity.

B. Electrical Measurements

1. Potential Type

In experimental work on electrochromic devices, triangle or ramp potentials are commonly used. They are generated from a potentiostat. However, in practice, a square wave or dc potential is used on commercial devices. Current is generally limited by the driving supply. This is necessary because these devices go through large impedance changes when they color and can be over-driven if the current is not limited. In some coloration studies stair-step potentials are used. In general, different potentials are used for bleaching and coloring. Also, pulse potentials are used to limit current.

2. Injected Charge Measurement

The amount of injected charge is usually reported as surface density of charge, charge per unit area, or charge density. Injected charge is calculated by integration of the current with respect to time. Also, a coulometer can be used to simplify measurements. One method to determine the injected/extracted charge and its relationship to injected/extracted ions of an electrode is voltametric titration (Yu, 1991). The dynamics of the charge-discharge characteristics of an electrode relating to ionic diffusion can be determined from chronopotentiometry, as discussed in Section 4. An important issue concerns the definition of surface density of charge. Surface density of charge (mC/cm^2), charge per unit area (mC/cm^2), and true charge density (mC/cm^3) are reported by various investigators. True charge density can also be reported as mC/cm^2 per nanometer of film thickness. To further confuse the issue, surface density of charge is sometimes reported as charge density. It is important to realize that what one is measuring has a physical meaning with respect to the device geometry. The preferred terminology is surface density of charge (mC/cm^2).

Charge capacity (mC/cm^2) is another vague term. It refers to the amount of charge stored or extracted per cycle for either an electrode or a device. Unfortunately, in diffusion controlled reactions the injection rate will play a role in the determination of charge stored or extracted so the sweep rate must be specified. To determine charge capacity, slow sweep rates are used, such as 2mV/s, to obtain a quasi-steady-state condition. A method to obtain charge capacity employed is to integrate a voltammetry or current-voltage (IV) plot operating within a safe potential region for the electrode or device. The safe potential region avoids any gas generation or decomposition potentials and should obey a balanced charge-potential relationship for each electrode used in the device. Depending on the material and its microstructure, charge capacity may or may not have linear relationship to thickness over some range of film thickness. The charge capacity of an electrode can be related to a theoretical capacity, such as is done with batteries. The ratio between actual and theoretical values is called electrode utilization.

3. Voltammetry and Current-Voltage Characteristics

Voltammetry is used to determine the basic electrochemical IV characteristics of an electrochromic electrode or device. In voltammetry the driving waveform is a triangle potential with reference to a standard reference electrode. The voltammetry potentials can be related to electrochemical processes, such as redox reactions occurring at the electrode. Voltammetry is used extensively in cyclic studies of electrodes in liquid and semi-solid electrolytes. Prototype devices seldom have the provision for a reference electrode. However, in certain constructions, a reference electrode can be made by introducing a thin electrode into the ion conductor layer provided it can be electrically isolated. Since many devices do not use reference electrodes, researchers only report IV characteristics.

4. Switching Chronopotentiometry

Numerous electrochemical techniques have been developed for the analysis of electrode kinetics, especially for battery electrodes. Voltammetry, chronoamperometry, and chronopotentiometry are the most widely used methods. For electrochromic electrodes voltammetry is the most widely used technique. Chronopotentiometry is used to help determine the transport characteristics of an electrochromic electrode. There is no rigorous analysis of the electrode kinetics of solid-state electrochromic films involving redox reactions. This has been due in part to the difficulty in the analysis of finite diffusion in the film. Since electrochromic films change color as a result of injected or ejected charge, chronopotentiometry is a very important technique for the study of charge/discharge characteristics under constant current. Chronopotentiometry is an electrochemical technique in which a current step is applied to the electrode and the potential response of the system is recorded as a function of time. If the flow of the current is reversed after a certain time period and electrolysis is continued, then it is called switching chronopotentiometry.

5. Impedance Spectroscopy

Electrochromic devices exhibit complex impedance properties which are non-linear and ion (charge) injection dependent. Impedance spectroscopy is an ac. technique and for electrochemical materials has been found to be superior to the classic dc method. The dc impedance technique does not work well for electrolyte media with low conductivity where fairly large dc signals are required which cause polarization and can interfere with the measurement. ac. electrochemical impedance spectroscopy has been used to analyze the ionic and electronic transport components of conductivity and electrode corrosion rate in materials such as battery electrodes and ionic conducting polymers (Madonald, 1987). Electrochemical impedance spectroscopy can be used to characterize electrochromic materials. However, this technique is relatively new and has mainly been used by electrochromic researchers developing polymer electrolytes or studying electrode characteristics (Nagai, 1983). In this measurement technique, a voltage of variable frequency is applied to interfaces. One measures the phase shift and amplitude of the resulting current; depending on the type of materials studied, the frequency domain may vary but, generally, measurements are done from 1mHz to 30MHz. The relationship between applied voltage and current flow is impedance, which is analogous to the resistance-current potential relationship of a dc measurement. To accomplish this measurement, a correlation frequency response analyzer and an electrochemical potentiostat interface are used. Because of the large amount of data generated, computer control with data storage is required. The frequency response analyzer generates the ac signal and measures the response from the device as ratios of current and voltage to the applied signal. The potentiostat interface provides control over the cell during the measurement.

The parameters derived from impedance spectroscopy include: conductivity, charge mobility, equilibrium concentrations of the charged species, capacitance of the interface region, and the diffusion coefficients of different species into the electrode. Nagai et al., (1983), for example, have applied impedance analysis to characterize ITO and Li_xWO_3 electrodes for electrochromic devices. By this method, the authors estimated electrochemical parameters such as the capacitance of the double layer, the charge transfer resistance of the electrolyte solution, and the diffusion coefficient of lithium ions in Li_xWO_3. To derive these physical parameters from impedance measurement one must devise an equivalent circuit model for the electrochemical system. The impedance of the various elements in the circuit model are derived by using circuit analysis. Software for circuit analysis has been developed for polymer electrolytes and certain electrochemical systems.

To our knowledge, there is no established or standardized method to adequately analyze the results of impedance spectroscopy in all inorganic solid-state devices using ion conductors. Expressions for the impedance in situations where liquid electrolytes are used can not be transferred unchanged to the solid-state cases. The difference between solid state and liquid electrolytes is discussed in detail by Raistrick et al, 1987, who noted that empirical and semi-empirical models have been advanced by many authors for solid-state interfaces. Impedance spectroscopy is, however, a powerful technique and its usefulness should not be overlooked. If properly developed, it can give valuable information about electrochromic device characteristics, from intrinsic properties of the device components to parameters related to important device properties.

6. Point-of-Zero-Zeta-Potential Measurement

The use of metal oxides for electrochromic windows has attracted considerable interest. One thing that is lacking in the design of electrochromic devices is a predictive technique to determine the compatibility of metal oxides used with various electrolytes and solid-state ion conductors. Here we present a useful technique to evaluate electrochromic materials.

The optical, electrical, and material transport properties depend strongly on the microstructure of metal oxides. Also, electrochromic activity is affected by the state of H^+ and OH^- ions at oxide surface. Very few studies are known on the surface characteristics of metal oxides and ions. Below, the concept of the Point-of-Zero-Zeta-Potential (PZZP) and its application (Krolov, 1970, Butler, 1978) is presented.

The concept of PZZP was developed by M.A. Butler et al., 1978. The PZZP is the pH at which the net surface charge is zero or the concentration of absorbed OH^- and H^- ions is equal. Several techniques have been used to determine PZZP's. The simplest is potentiometric titration, involving the addition of the metal oxide powder into an aqueous solution of a known pH. Titration of the oxide suspension with either acid or base gives the PZZP. The pH of the solution will shift on addition of the acid or base towards the PZZP. At the PZZP, the pH of the solution is not affected by excess oxide.

For an oxide with large value of X(M), the metal ion has a tendency to attract O- and weaken the bonding of O-H. Thus, the dissociation mode -M-O^-+ H^+ will be dominant. Increase in H+ causes a decrease in PZZP. It is well known that WO_3 is stable in acid environments and NiO is stable in alkaline solutions. This fact can be ascribed to each PZZP. For the selection of electrolyte, Ta_2O_5 is suitable for WO_3 but not for NiO. Therefore, it is necessary to adjust the chemistry of WO_3, NiO, and Ta_2O_5, which will alter the PZZP's, when solid state electrochromic devices are constructed from these materials. Even without experimental knowledge of PZZP, prediction of PZZP is possible from electron negativity, which acts as a guideline for electrode selection.

7. Cycle Power and Energy

The amount of power required for an electrochromic device varies during its coloration and bleaching cycle. An the beginning of each half cycle the instantaneous power is greater than the continuous power required; this is because of the non-linearity of the current. The cycle power (P) for an electrochromic device or electrode system can be calculated by integrating voltage V(t) and current I(t) over a period of the cycle. Also, the range of optical response should also be noted when cycle power is reported. Cycle energy is calculated by integrating V(t) and charge per cycle Q(t) or power and time per cycle.

It is very difficult to compare different materials and devices since their operating voltage, current and optical response are generally different. It is best to compare different materials and devices over a similar cycle of coloration. For example, energy consumption for a typical electrochromic is about 5 $\mu W\text{-}h/cm^2$ per cycle (10-70% peak transmittance change). For an

electrochromic device in operation, the actual energy consumption is very dependent on the number of daily cycles, the ranges of coloration, and the memory of the device.

C. Efficiency and Response Measurements

1. Coloration Efficiency

The coloration efficiency is a measure of how much charge is required to obtain a certain level of coloration. The coloration efficiency is very dependent on the material, its microstructure, and spectral characteristics. Typically, the coloration efficiency of an electrochromic electrode is measured from the change in optical density with charge Q at some specified wavelength.. Generally, the coloration efficiency (CE) is taken from the linear region of the $\Delta OD(l)$ verses Q relationship, using a graphical representation. An example is shown in Fig. 2. As one can see CE is not usually linear with wavelength over the visible region. Commonly, single values are reported for CE. Single values are only good for the wavelengths they were measured at and do not generally represent the entire visible or solar spectrum. Because of this problem one has to be very cautious when comparing CE's from different researchers. An alternative is to use an integrated value over the photopic spectrum for visible control. For solar control an integration over the solar region would be best.

The integrated coloration efficiency for solar (CE_S) and the photopic spectrum (CE_P) is:

$$CE_S = \frac{\int_{0.32\mu m}^{2.5\mu m} CE(l)\, I_S(l)\, dl}{\int_{0.32\mu m}^{2.5\mu m} I_S(l)\, dl} \qquad CE_P = \frac{\int_{0.39\mu m}^{0.77\mu m} CE(l)\, I_P(l)\, dl}{\int_{0.39\mu m}^{0.77\mu m} I_P(l)\, dl}$$

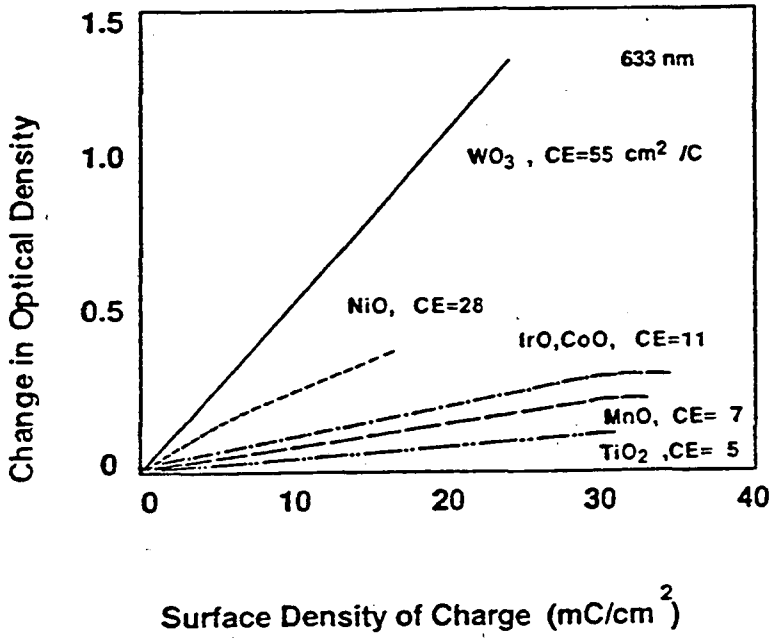

Fig. 2. Monochromatic Coloration Efficiency for different electrochromic metal oxides (Lampert and Granqvist, 1990).

2. Response Time and Memory Measurements

Currently, response times for electrochromic electrodes and devices are made monochromatically under somewhat arbitrary conditions determined by the investigator. In many cases, the peak coloration wavelength or 633 nm laser wavelength is used for this measurement.

Response time varies for each device and is strongly dependent on the conditions and levels of coloration and bleaching. The upper level of coloration is the hardest to specify. A proposed standard is to use 90% saturation for the upper bound for the colored condition. The lower bound should be 10% of the completely bleached (rest) state. An alternative would be to use two standard deviations from the saturated and bleached conditions, which are respectively 84% and 16% transmission. Another alternative is to define limits from d(ln ΔOD)/dt. The response time should be given for bleaching and coloration separately, using specific potentials. The duration of the applied potential and charge injection level is determined experimentally for each device type. It is important to give the dimensions of the working area of the device and the operating temperature. Also, it is useful to give the open circuit bleaching time, which will give a measure of natural bleaching and device memory (self discharge).

Memory is a measure of the electrochromic device's ability to stay colored over long periods of time. There are no standards for memory measurement. Some devices can have memory in excess of 24 hours. Devices with the best battery characteristics have the best charge storage and longest memory. Certain electrochromic devices self-discharge and have no appreciable memory. Memory should be measured according to the decrease in coloration to the bleached condition. It

is suggested that the colored condition be defined as 90% saturation and the bleached condition be 10% of the fully bleached rest state. An alternative would be to use two standard deviations from the saturated to bleached condition, which is 84% and 16% of the range.

D. Conclusions

This study addressed the issues of characterization and testing of electrochromic devices. Existing and new parameters to characterize electrochromic materials and devices were introduced. The parameters mentioned in this work were organized into three major areas: optical properties, electrical properties, and efficiency measurements. For optical properties, solar and photopic transmittance, reflectance, and absorptance; optical density; shading coefficient; and chromaticity coordinates were included. The determination of photopic and solar weighted values was discussed. Chromaticity coordinates were recommended for color description. The concept of shading coefficients needs to be developed for switchable materials.

For electrical measurements, potential type, injected charge, voltammetry and current-voltage characteristics, switching chronopotentiometry, impedance spectroscopy, point-of-zero-zeta-potential, and cycle energy and power were discussed. For charge injection measurements, the terminology is generally confused. We recommend that the term "surface density of charge" be used in place of charge density. Switching chronopotentiometry can be used to determine transport characteristics of electrochromic films. Impedance spectroscopy is a useful technique to determine various parameters, including ionic diffusivity and conductivity. Further work needs to be done to fully model impedance spectroscopy results for inorganic solid-state systems. Measuring the point-of-zero-zeta-potential is a useful technique for the characterization and selection of electrodes for devices. In the section on efficiency and response, the properties of coloration efficiency, response time, and memory were detailed. We recommend using spectral coloration efficiencies instead of monochromatic ones. We also recommend that 90% and 10% saturation be used as the limits for response time and memory measurements, though there are other possible limits. Finally, we recommend that further performance parameters relating to buildings (and vehicles) be developed to characterize the benefits of daylighting, solar energy control, and energy efficiency for heating and cooling.

E. References

Butler, M.A., and Ginley, D.S., J. Electrochem. Soc., 125(1978)228.

Czanderna, A.W. and Lampert, C.M., "Evaluation Criteria and Test Methods for Electrochromic Windows", Solar Energy Research Institute Report no. SERI-PR-255-3537, July 1990.

Krylov, O.V. Catalysis by Nonmetals, Academic Press, NY, 1970.

Lampert, C. M., "Electrochromic materials and devices for energy efficient windows," Solar Energy Materials 11(1984)1.

Lampert, C. M. and Granqvist, C. G., edits., Large-area Chromogenics: Materials and devices for transmittance control, Optical Engineering Press- SPIE, Bellingham, WA, (1990).

Lampert, C. M. , Truong, V-V., Nagai, J. and Hutchins, M. G., "Characterization parameters and test methods for electrochromic devices for glazing applications," IEA report, LBL-29632, (1991).

Lampert, C. M. Durability of Electrochromic Switching Devices for Glazings, Proc. of SPIE, 1272 (1990)56.

MacAdam, D. L. Color Measurement, 2nd. edit., Springer-Verlag, Berlin, Germany, 1985.

Mcdonald, J. R., Impedance Spectroscopy, John Wiley, NY, 1987.

Murdoch, J. B., Illumination Engineering, Macmillian, NY 1985.

Nagai, J., Kamimori, T. and Mitzuhashi, M., Application of impedance spectroscopy analysis to the characterization of ITO and Li_xWO_3 electrodes. Reports of the Research Labs, Asahi Glass Co. 33 (1983)99-116.

Raistrick, I. D., Mcdonald, J. R., Franceschetti, D. R., in Impedance Spectroscopy, Mcdonald, J. R., Edit., Wiley, NY, pp. 101-132, 1987.

Reilly, S. Arasteh, D. and Selkowitz, S., "Thermal and optical analysis of switchable window glazings", Solar Energy Mat. 22(1991)1.

Simon, R. E., Electrooptics Handbook, RCA Corp., Lancaster, PA.,1974.

Yu, P. C., "Characterization of Indium Sesquioxide and Niobium Pentoxide for the Application as Counter-Electrodes in and Electrochromic window, Ph.D. Thesis, Tufts University, Dept, of Chemistry, Medford, MA, May 1991.

III. MEASUREMENT OF THE ASAHI PROTOTYPE ELECTROCHROMIC WINDOW

C. M. Lampert, M.G. Hutchins, G. McMeeking, V.-V. Truong, P. V. Ashrit, F. Aleo, P. Carbonaro, A. Ferriolo, S. Tanemura, W. Platzer, V. Wittwer and J. Klems.

A. Introduction

One of the most famous prototype electrochromic windows was investigated. Several 10-cm x 10-cm windows were provided by Dr. Nagai of Asahi Glass (Yokohama, Japan) and distributed to the members of the study group. A special power supply was provided by Asahi Glass. It had preset values for voltage, current, and the duration of each cycle. This was for consistency of measurement and to prevent the evaluators from overdriving the devices. In some of the experiments, the following parameters were used to power the devices: rest state = 0 V; colored state = 2.0 V, 60 mA for 25 s; bleached state = –0.7 V, 60 mA for 100 s. The positive potential was taken relative to the tungsten oxide layer. (Tungsten oxide cathodically colors when a negative potential is applied).

The Asahi electrochromic window was designed to use Li^+ ions for coloration of amorphous WO_3, with a redox couple as part of a semi-solid electrolyte (Nagai, 1986; Mizuhashi, Nagai, and Kamimori, 1990). The problem associated with the use of liquid electrolytes has been reduced by using UV or thermally curable acrylic polymer as a binder (Nagi, Kiyoya, and Kamimori, 1989). This development has made the use of liquid phases useful to the manufacture of large-area devices. About 200 prototype electrochromic windows (30 cm x 30 cm in size) of the same type have been installed in the Seto Bridge Museum (Kojima, Okayama-Pref., Japan). Also, another 50 windows have been installed in the Daiwa House (Mita-city, Hyogo-Pref., Japan). The experiments performed on these windows by our subtask group were mainly optical evaluations under different conditions. Considerable experience was gained by our group in the use of spectrophotometers and the characterization of switchable glazings, as most of the participants were only familiar with materials with fixed properties. Under a joint project between Lawrence Berkeley Laboratory (LBL) and Asahi, we measured thermal heat flows in a matrix of 9 30-cm x 30-cm electrochromic panes in the mobile thermal test facility (MoWiTT) at Reno, NV, USA. Those results give an indication of the amount of energy savings possible with electrochromic glazings. Such savings could be as large as 30–50% compared to conventional windows.

B. Experimental Conditions

In Europe, the Italian group at Conphoebus used a Varian Cary-2400 spectrophotometer with a 60 mm integrating sphere coated with Teflon. The incident angle was near-normal to the sample surface and measurements were relative to the sphere coating. Also, measurements to characterize the dynamic properties of hazing and fading phenomena of the sample were performed. Instrument settings were: scan rate of 5.0 nm/s with a response time of 3.0 s for spectral transmittance measurements. The German group made spectral measurements over the solar wavelength region (300-2500 nm) using a Perkin-Elmer Lambda-9 spectrophotometer. Total transmittance, total reflectance, and diffuse reflectance were determined using an 150 mm integrating sphere from Perkin-Elmer coated with barium sulfate. The detectors are shielded

from the ports for the reference standard and the reflecting sample. However, the detectors in this sphere are not shielded with baffles against the input port; therefore, the total transmittance might be overestimated. A light trap was used to exclude background radiation through the partly transparent samples. Halon was used as the reference standard. The plotted curves are corrected using the calibration data from the sphere supplier (Labsphere). The UK group made near-normal direct spectral transmittance measurements over the spectral range 2500-300 nm for both the bleached and colored states of the device. They used a Beckman 5270 dual beam ratio recording spectrophotometer. The UK Group used bleached and colored state voltages of +0.7 V and -1.4 V, respectively.

In North American, the Canadian group used a Cary 2400 (UV-VIS-NIR) spectrophotometer to measure near-normal properties over the 300-2500 nm range. The U.S. group used a Perkin Elmer Lambda 9 Spectrophotometer to determine near-normal values of transmittance for the 300-2500 nm range.

The Japanese group at NIRI-Nagoya used a HITACHI 3400 type spectrophotometer with integrating sphere of 60 mm in diameter coated with $BaSO_4$. The incidence angle was near-normal to sample surface and transmitted beam impinged on a part of the sphere. Six designated wavelengths for the measurement of time dependent normal-hemispherical transmittance were 0.707, 0.667, 0.630, 0.593, 0.555, and 0.519 μm. Two Asahi devices were tested to characterize the optical properties. One was supplied by Asahi Co. directly (labeled as Sample 1) and the other by C. Lampert (labeled as Sample 2). Sample 1 was used for the measurement of normal-hemispherical spectral transmittance for colored and bleached state. Sample 2 was used to determine time dependent normal-hemispherical transmittance at six designated wavelengths after the removal of the applied voltage. This measurement was performed to determine fading or memory of the device. All the participants calculated integrated values from Air Mass 1.5 solar data using the ASTM E891 standard or ISO standards.

C. Results

In order to measure the correct optical transmittance both in bleached and colored state, a steady dark and bleached state should be obtained. The bleached state and the rest state are not the same. In Fig. 1 is shown a set of spectral transmittance measurements made by the German group. Comparative results are shown in Table 1 for the other groups. Shown in Fig. 2, is the coloration rate at 550 nm under a constant voltage of 0.75V (from the Canadian group). Notice that after about 2 minutes the coloration tends to saturate to about 10% transmittance. The open circuit memory, starting from a fully colored condition, is shown in Fig. 3. This window shows fairly rapid fading from the first 5 minutes (0.10 to 0.30 transmittance), see Fig. 4. Afterwards, the window continues to fade but much more gradually. The reflectance ranged from 0.11-0.16 in the devices over the solar spectrum from bleached to colored. The colored state had the lowest reflectance. The majority of the color change was caused by absorptance. Further data can be found in our Task 10C Working Document (Hutchins, 1990).

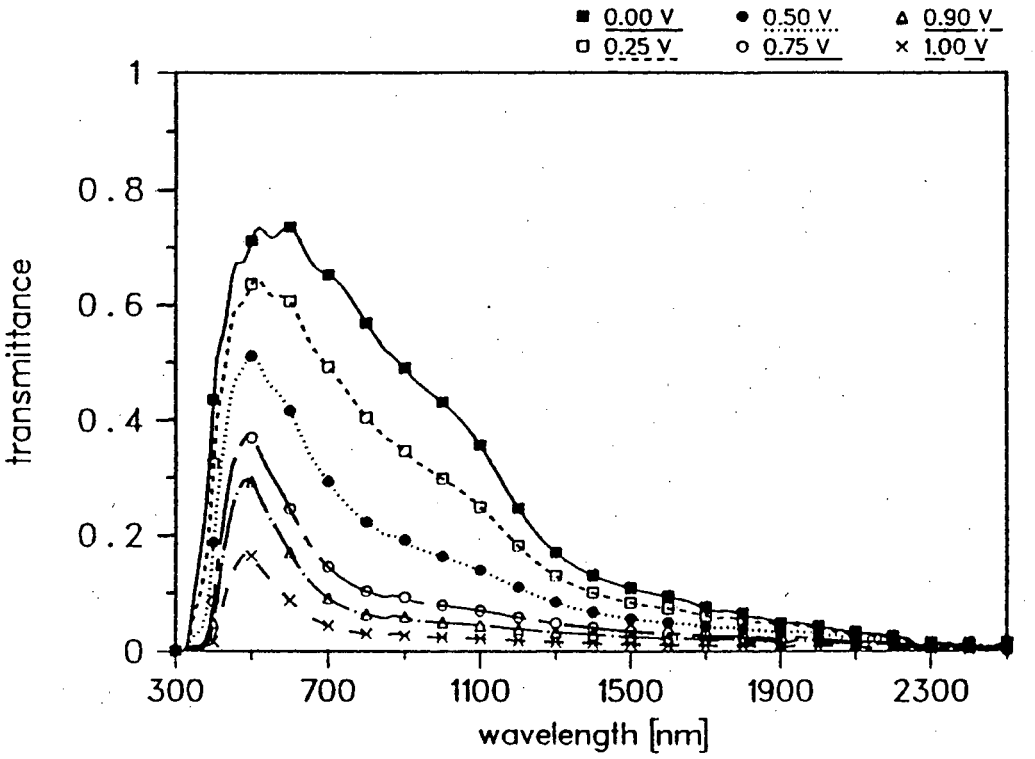

Fig. 1. The spectral transmittance properties of an Asahi 10 cm x 10 cm prototype electrochromic window under several voltage conditions (0.0-1.0V).

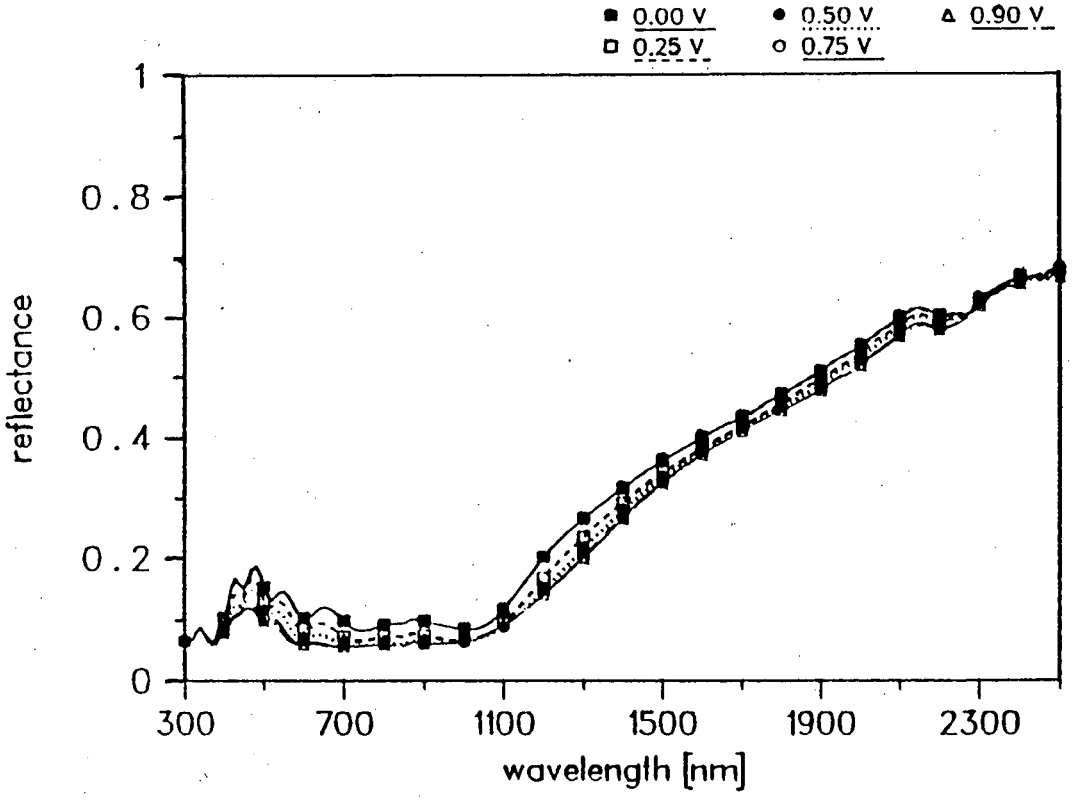

Fig. 2. The total spectral reflectance properties of an Asahi 10 cm x 10 cm electrochromic window under several voltage conditions (0.0-0.9V).

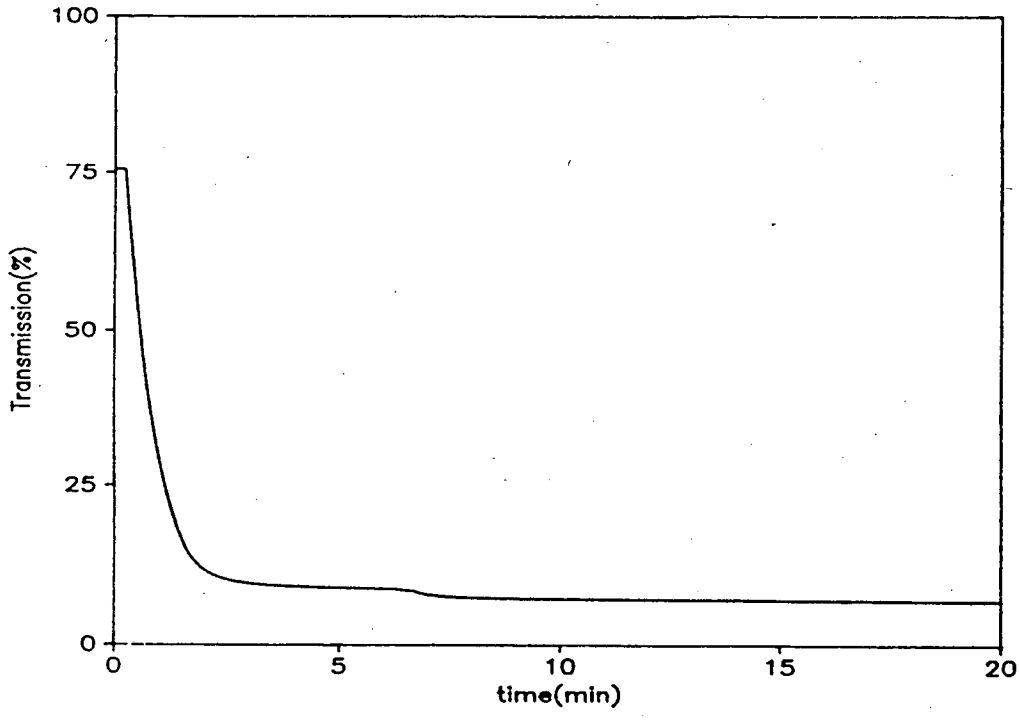

Fig. 3. The coloration rate of an Asahi 10 cm x10 cm electrochromic window powered at 0.75V, 10 mA.

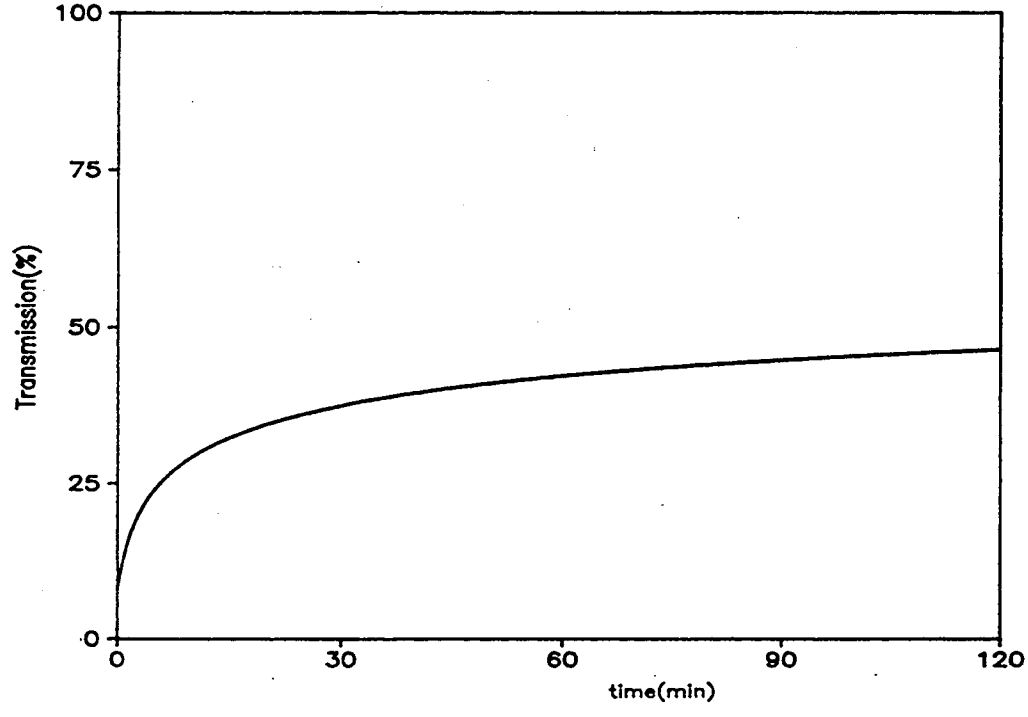

Fig. 4. The fading rate or memory of an Asahi 10 cm x 10 cm electrochromic window colored at 0.75V, 10 mA and allowed to go to open circuit conditions.

Table 1. Asahi Window Optical Properties

Measurement	Italy	USA	UK[c]	Japan 1	Japan 2[b]	Canada[a]	Germany[b] (T&R, Total)
Rest State (solar)	0.422	0.424				0.488	
Rest State (photopic)	0.646	0.656				0.764	
Colored (solar)	0.011	0.015	0.097	0.042	0.056	0.073	0.058(R=0.118)
Colored (photopic)	0.033	0.038	0.207			0.166	0.115(R=0.074)
Bleached (solar)	0.529	0.505	0.533	0.533	0.5164	0.563	0.501(R=0.159)
Bleached (photopic)	0.764	0.756	0.785			0.836	0.719(R=0.130)
Rest State solar value (after 2 days, 0V)	0.471						

a) Coloration was obtained with 0.8V and bleaching at -0.7V.
b) Coloration potential was 1.0V, with saturation current below 10 mA. For Japan, it was at 7.46 mA (start) and 7.20 mA (stop). The time required for current saturation was 31 minutes.
c) Bleaching potential was 0.7±0.1V and coloring potential was -1.4±0.1V.

Notes: Most devices were powered by -2.0V to color over 25 s with current limited to 60 mA. Devices were bleached at 0.5V over 100 s with current limit of 60 mA. The rest state is the initial state of the device after no cycling for over 24 hours. Note that the bleached state and the rest state are not the same. The bleached state is more colored than the rest state. All the participants calculated integrated values from Air Mass 1.5 solar data using the ASTM E891 standard or ISO standards. The integrated photopic response was calculated from the standard CIE/ISO photopic spectra.

The UK group made measurements of color on the electrochromic window. In the bleached condition ($T_p = 0.785$) the coordinates were: x = 0.3179, y = 0.3343, and z = 0.3478, with D_λ = 484 nm and E_p = 35%, for Illuminant A. For the colored condition ($T_p = 0.207$) the coordinates were: x'= 0.2498, y' = 0.2992, and z' = 0.4510 with D_λ =484 nm and E_p= 52 %.

Chromaticity Coordinates	x	y	z	Visual Efficiency
Bleached	0.3179	0.3343	0.3478	77.7%
Colored	0.2498	0.2992	0.4510	20.4%

Notes: All devices were powered by -2.0V to color over 1 minute with current limited to 250 mA, device were bleached at 0.5V over 2 minutes with current limits of 250 mA.

D. MoWiTT Energy Evaluation

Work is on-going at LBL to evaluate the thermal and daylight control properties of the Asahi electrochromic window using the MoWiTT mobile window test facility (Klems, 1984, Klems, 1989). The MoWiTT consists of two side-by-side room-sized, guarded calorimeters that measure net heat transfer through two window systems over relatively short time periods under non-steady state conditions. The MoWiTT can be used to determine U-values and thermal performance (for both day and night conditions) and solar heat gain. These window systems are simultaneously exposed in the same orientation and ambient weather conditions. Energy performance data are shown for a 3 x 3 matrix of 30 cm x 30 cm Asahi electrochromic windows compared to a bronze single glazed window in Fig. 5. The electronically controllable window has a considerable energy advantage over that of a conventional bronze window. In this test the daylight illumination level inside the test chamber was regulated by the window to a constant value (50 fc), see Fig. 6. Energy modeling has shown that electrochromic windows can provide significant energy performance over that of conventional double glazed windows (Reilly, Göttsche and Wittwer, 1991).

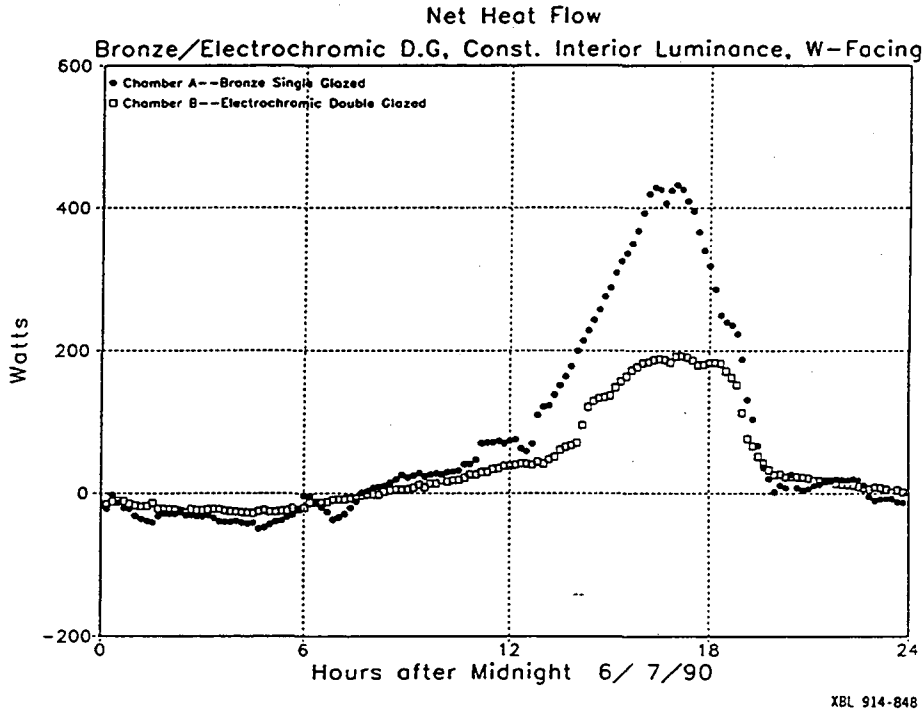

Fig. 5. Energy performance data is shown as net heat flux for a 3 x 3 matrix of 30 cm x 30 cm Asahi ECW electrochromic windows compared to a bronze single glazed window. This heat flux corresponds to a control of the lighting level in the chamber to 50 fc (see Fig. 6).

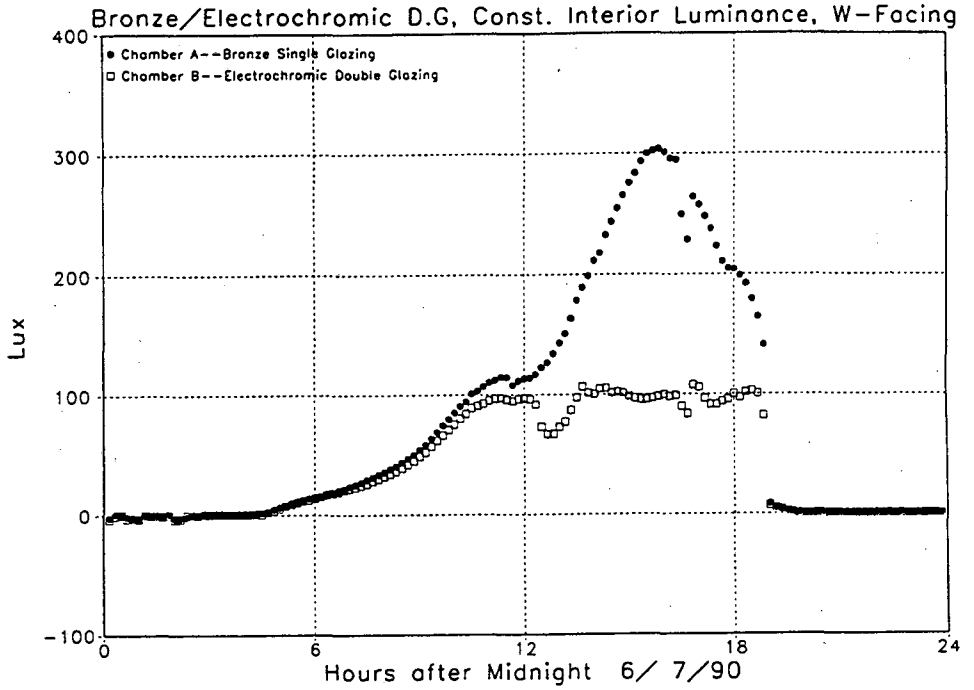

Fig. 6. Net light transmittance data for a 3 x 3 matrix of 30 cm x 30 cm Asahi ECW electrochromic windows . The interior light level was set at to 50 fc.

E. References

Hutchins, M.G. "Optical properties of liquid crystal devices" IEA Working Document, Oxford Brooks University, Oxford, UK, (1990).

Klems, J. L. "Measurement of fenestration net energy performance considerations leading to development of the MoWiTT," J. Solar Energy Engin. 110(1984)208.

Klems, J. L. " U-Values, solar heat gain, and thermal performance: Recent studies using the MoWitt", ASHRAE Proc. Jan 29-Feb., 1989.

Mizuhashi, M., Nagai, J. and Kamimori, T. "Electrochromic device design toward large-scale applications" in Large-area Chromogenics: Materials and devices for transmittance control, (Lampert, C. M. and Granqvist, C. G., edits.) Optical Engineering Press- SPIE, Bellingham, WA, (1990)494.

Nagai, J., Kamimori, T., and Mizuhashi, M., "Transmissive electrochromic device," Solar Energy Mat. 14(1986)175.

Nagai, Y., Kiyoya, T. , and Kamimori, T. "Electrochromic elements," JP 63,249,826, 1 Sept. 1989.

Reilly, S., Göttsche, J., and Wittwer, V.," Advanced window systems and building performance," Proc. ISES, Denver, CO, July (1991) 3211.

IV. OPTICAL CHARACTERIZATION OF THE TALIQ LIQUID CRYSTAL WINDOW

P. van Konynenburg, M. G. Hutchins, G. McMeeking, U. Frei, C. M. Lampert,
V.-V. Truong, W. Platzer, V. Wittwer and B. Karlsson.

A. Introduction

Liquid-crystal-based systems offer another approach to chromogenic, electrically activated devices. The basic classes of liquid crystal light switching devices are the twisted nematic, guest-host, surface stabilized ferroelectric, and phase dispersed liquid crystals. The mechanism of optical switching in liquid crystals is to change the orientation of liquid crystal molecules interspersed between two conductive electrodes with an applied electric field. The orientation of the liquid crystals changes with the field strength. The movement of the liquid crystal alters the optical properties of the device (Chandrasekhar, 1977; de Gennes, 1974; Blinov, 1983). Open circuit memory is not possible with liquid crystals.

The phase dispersed liquid crystal (PDLC) or nematic encapsulated liquid crystal (NCAP, or nematic curvilinear aligned phase) consists of nematic liquid crystals distributed in microcavities (Drzaic, 1986). This cavity structure can give modulated light scattering known as the Christiansen effect. PDLC and NCAP materials have very similar characteristics but are defined differently in the patent literature according to their preparation procedure. The NCAP films are formed from an emulsion, and PDLC films are formed from an isotropic solution which phase separates during curing. General Motors Research Laboratory, Kent State University (Kent, OH), and 3M (St. Paul, MN) are developing PDLC technology for automotive glazing (Montgomery, 1990). Currently, plans for production of glazing devices are being made.

Devices based on NCAP technologies are being produced by Taliq (Mountain View, CA, USA) as optical shutter materials for glazings and information displays (known as Varilite and Vision Panel). Varilite is the type of material measured in this study. These products are now produced by Raychem Corp., Display Products Group, Sunnyvale, CA. Nippon Sheet Glass markets this product in Japan as the UMU Device, and Saint-Gobain, La Defense, Paris, France. At least two other major companies in the U.S. are developing NCAP automotive sunroofs. Large-area devices have been fabricated in 1-m x 2.5-m sheets.

With NCAP, the liquid crystals are encapsulated within an index-matched polymer matrix. The composite polymer is fabricated between two sheets of ITO-coated polyester that serve as electrodes. The device can also be fabricated between one sheet of glass and one sheet of plastic or between two sheets of conductive glass. The switching effect of this device spans the entire solar spectrum, up to the absorption edge of glass. In the off state, the device appears translucent white. Since the off state in these devices is diffusely transmitting, the device has application for privacy and security. When an electric field is applied, the liquid crystal droplets align with the field and the device becomes transparent (Fergason, 1985).

Typically, these devices operate between 0 and 100 V ac, but they switch most strongly from 30 to 70 V ac. They comsume less than 20 W/m^2 power, but they have no memory and require continuous power to stay clear. Pleochroic dyes can be added to darken the device in the off

state (van Konynenburg, Marsland, and McCoy, 1989). One experimentally dyed film was investigated in this study (sample 00430). In general, compared to electrochromics, the power consumption is higher because of the need for continuous power in the activated state.

Dispersed liquid crystal devices have a very bright future but are restricted by three characteristics: the unpowered state is diffuse, haze remains in the activated (transparent) state, and UV stability is poor. Many of the devices made to date are used in interior building applications. The residual haze problem can probably be alleviated by better control over the formation and processing of the liquid crystal emulsion. The UV stability of the NCAP and PDLC materials will improve with understanding of failure mechanisms and with materials improvements. For widespread use of NCAP devices, the cost will have to decline.

B. Experimental Conditions

Three samples of the Taliq NCAP product known as Veralite were evaluated by the IEA SHC group. Peter van Konynenburg of Taliq (now with RayChem) provided the group with samples. Two were undyed and one dyed for automotive solar control use. Of the two undyed films, type 106A has lower haze (higher clarity) than type 305B film. The dyed film was designated as 00430 and it was measured only by a few laboratories This study involved the determination of the spectral near-normal, hemispherical, and scattering data over the solar and visible spectra as a function of voltage.

The U.S. group used a Guided Wave (El Dorado Hills, CA, USA) fiber optic spectrophotometer, model 260. All analysis was done in the normal transmission mode. A 5 mm beam diameter was used in a normal transmission mode for analysis. Each sample was powered by a variable voltage source from 0-90 V ac. Data were taken at 10-V intervals. The respective transmittance values are denoted by $T_{voltage}$, where the voltage was 0-90V. After the highest voltage, 90V the sample was returned to 0 V. We noticed a slight change (0.3% increase) in the $T_p(0)$ transmittance compared to the initial value. Also, scattering measurements (not shown here) were made by the Swedish participant. The Canadian, Italian, German, and UK groups used the same equipment described in the Asahi electrochromic measurements, except the UK group used an integrating sphere. The UK reference material was barium sulfate. The PDLC devices were powered using a function generator. For the measurements by the German group, the detectors in their sphere were not shielded with baffles against the input port. Therefore, the total transmittance might be overestimated. This effect, is probably negligible since the Taliq samples show mainly forward scattering and the scattered intensity does not enter the detector ports directly.

Also, the German team made scattering experiments. The angular distribution of scattered intensity has been determined with a spectrogoniometer with low angular resolution. A Xenon-Arc-lamp is used as a source. The incident light on the sample is filtered by a double-monochrometer. A beam splitter in front of the sample is used to record the intensity with a monitoring photocell. The sample is mounted on a rotatable holder, therefore, the sample orientation determines the incidence angle. An 1 mm thick photodiode detector can be rotated (by a stepping motor) approximately 200 degrees around the sample at an distance of 10 cm. For the scattering experiments, the light beam hits the sample at normal incidence. The detector is

moved 180 degrees from the direction of the incident beam (0 degree) to the direction opposite (outgoing beam without sample). In this way, reflected and transmitted intensity is recorded except the specular reflected part at the 0 degree position because there the detector shaded the sample. There was no noticeable change of scattered intensity with polarization of the incoming beam. The scattering data were scaled to the spectrophotometer transmittance measurements. The signal was corrected for a small amount of background noise.

C. Results

A typical hemispherical transmittance spectrum is shown for the low-haze liquid crystal sample (106A) in Fig. 1. The net transmittance changes very little between 0 and 100 Vac, but the degree of scattering changes greatly. Overall, the spectral response is very broad compared to other types of switching films. In Fig. 2 the spectral response for a dyed film (sample 305B) is shown. Here the response is particularly enhanced in the visible region compared to the undyed film in Fig.1. The majority of the switching occurs between 10 and 50 V. The change in hemispherical transmittance is shown as a function of voltage for the dyed film is shown in Fig. 3. In this figure you can see that the largest change is between 30 and 70 V ac. From 70-100 V, very little change in the spectra is noted. In Fig. 4 the spectral hemispherical diffuse transmittance is shown for the dyed film. Note the complex visible response. This response is shown as a function of voltage in Fig. 5. An interesting rise in diffuse transmittance between 30-60 V ac is seen. This effect is not easily explained, but it may have to do with dye molecules oscillating in the field. In Figs. 6 and 7 the hemispherical total and diffuse solar transmission of the dyed and undyed films are compared. The dyed films show a substantial change in total transmittance compared to the undyed films. The corresponding data are shown in Tables 1 and 2. Table 1 shows the total and Table 2 shows the diffuse transmission results from all the participants. Both the US and Germany groups made specular measurements which are shown in Table 1. All the participants calculated integrated values from Air Mass 1.5 solar data using the ASTM E891 standard or ISO standards. The integrated photopic response was calculated from the standard CIE/ISO photopic spectra.

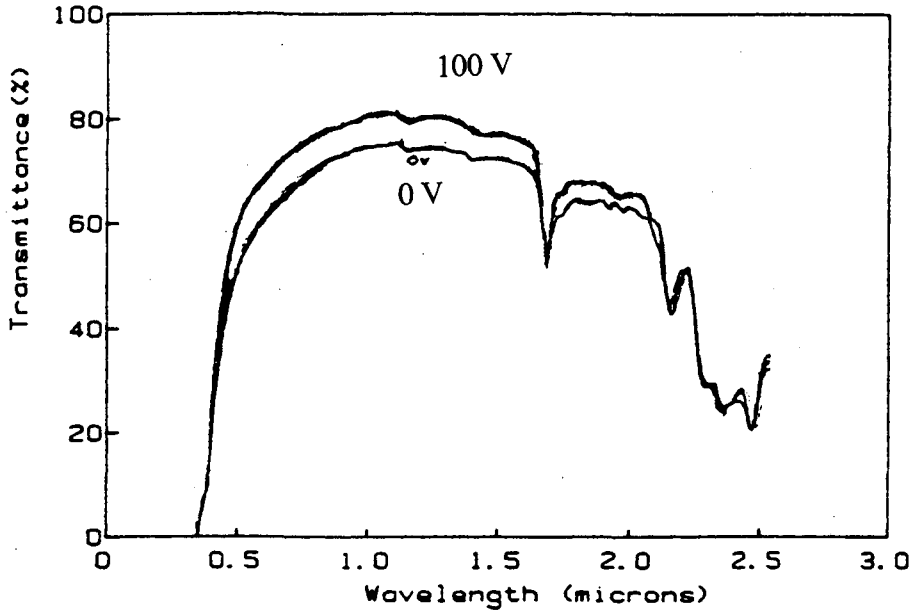

Fig. 1. Near-normal hemispherical transmittance of an undyed Taliq liquid crystal window film (type 106A). Both the fully transparent (on at 100 V ac) and fully scattering (off at 0V) conditions are shown. The color is translucent white when off.

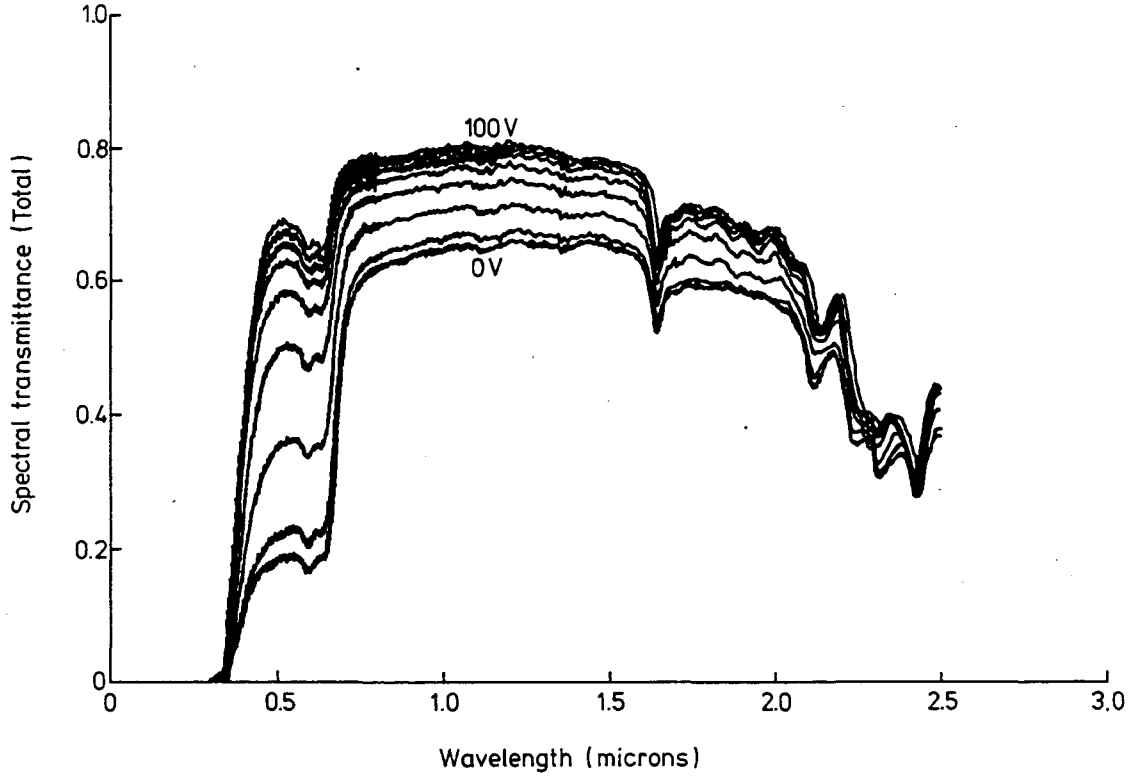

Fig. 2. The near-normal hemispherical transmittance properties of a Taliq dyed NCAP window (type 00430). Increments of 10Va. c. are shown in the figure from 0V to 100V ac. The color is gray.

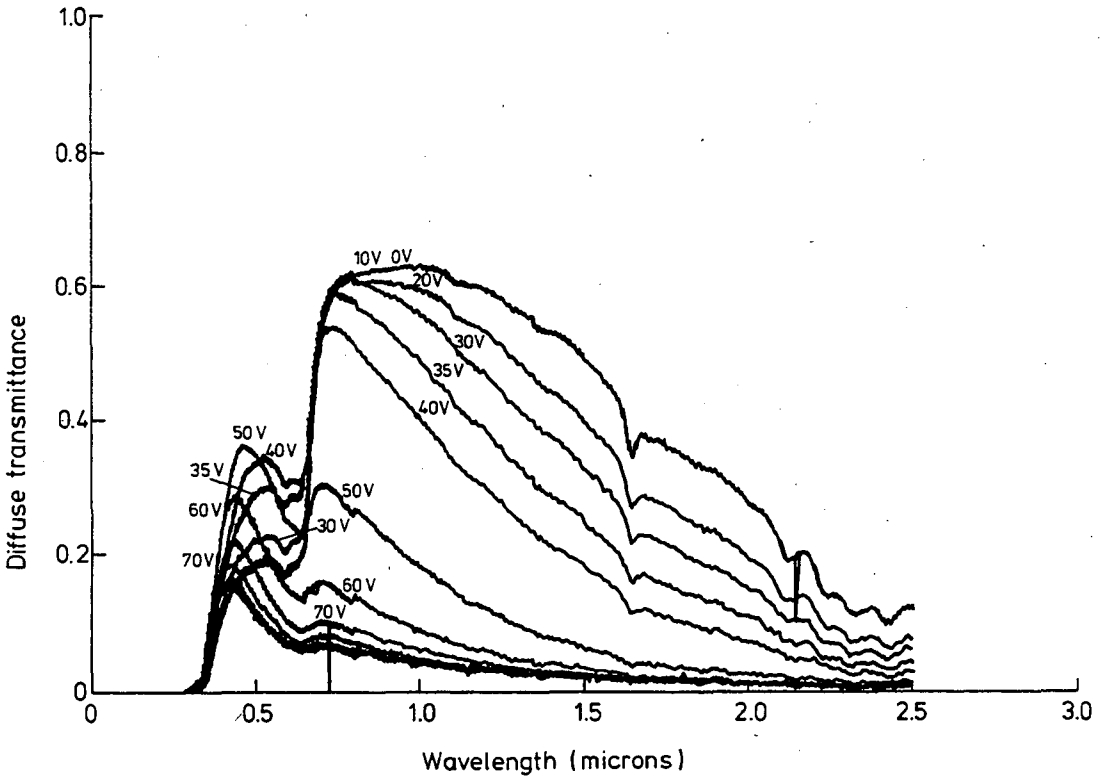

Fig. 3. Near-normal hemispherical diffuse spectral transmittance for dyed Taliq liquid crystal film (type 00430) for applied voltages in the range 0 - 100 Vac.

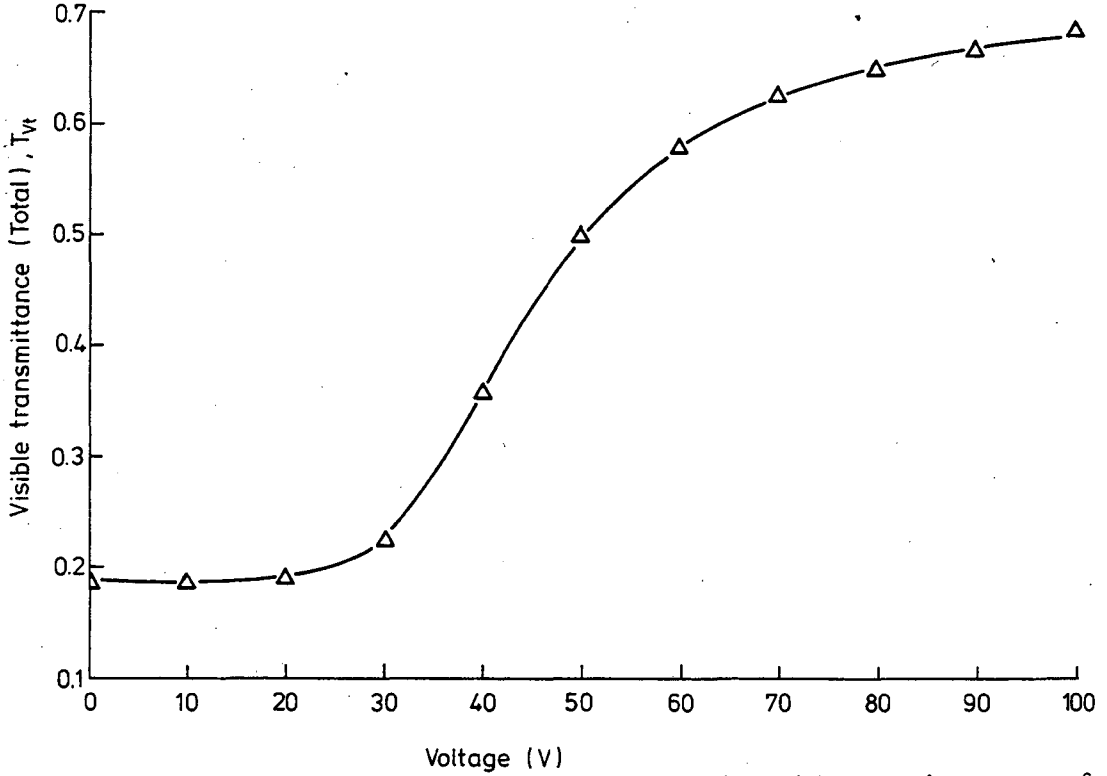

Fig. 4. Integrated near-normal hemispherical total visible (photopic) transmittance as a function of applied voltage for the Taliq dyed liquid crystal film.

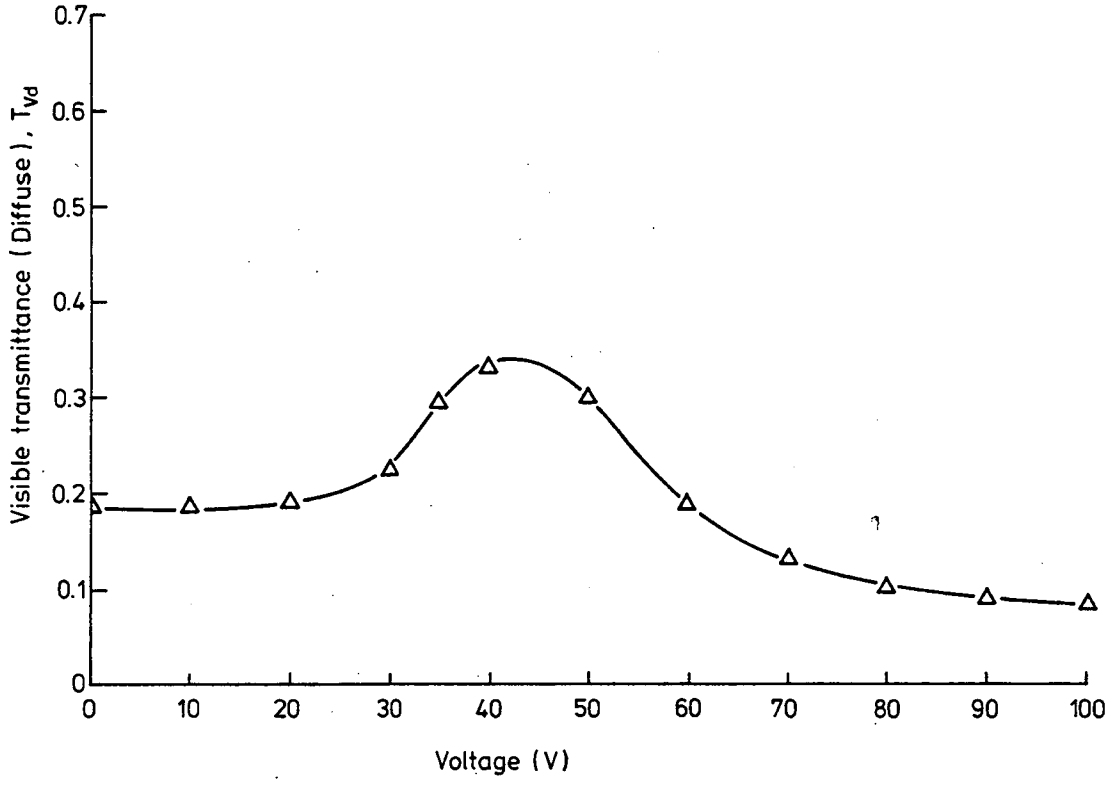

Fig. 5. Integrated near-normal hemispherical diffuse visible (photopic) transmittance as a function of applied voltage for the Taliq dyed liquid crystal film.

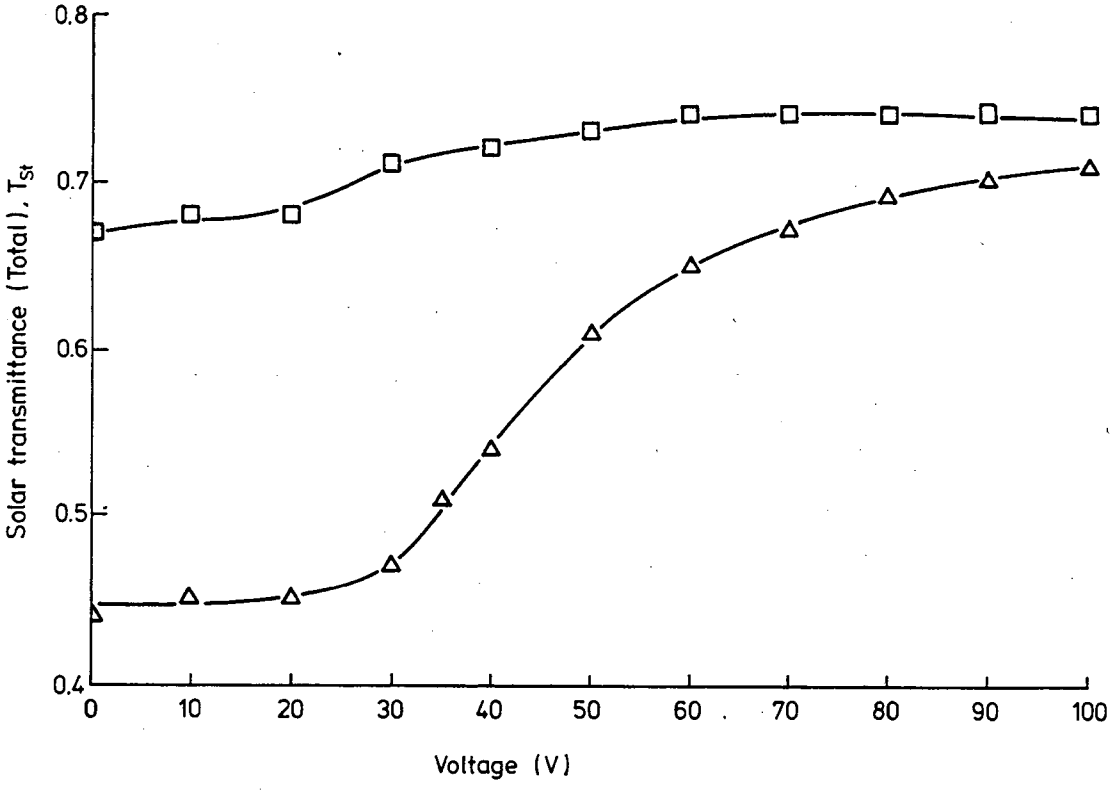

Fig. 6. Comparison of the integrated near-normal hemispherical total solar transmittance values of the dyed (triangle) and undyed (square) Taliq liquid crystal film as a function of applied voltage.

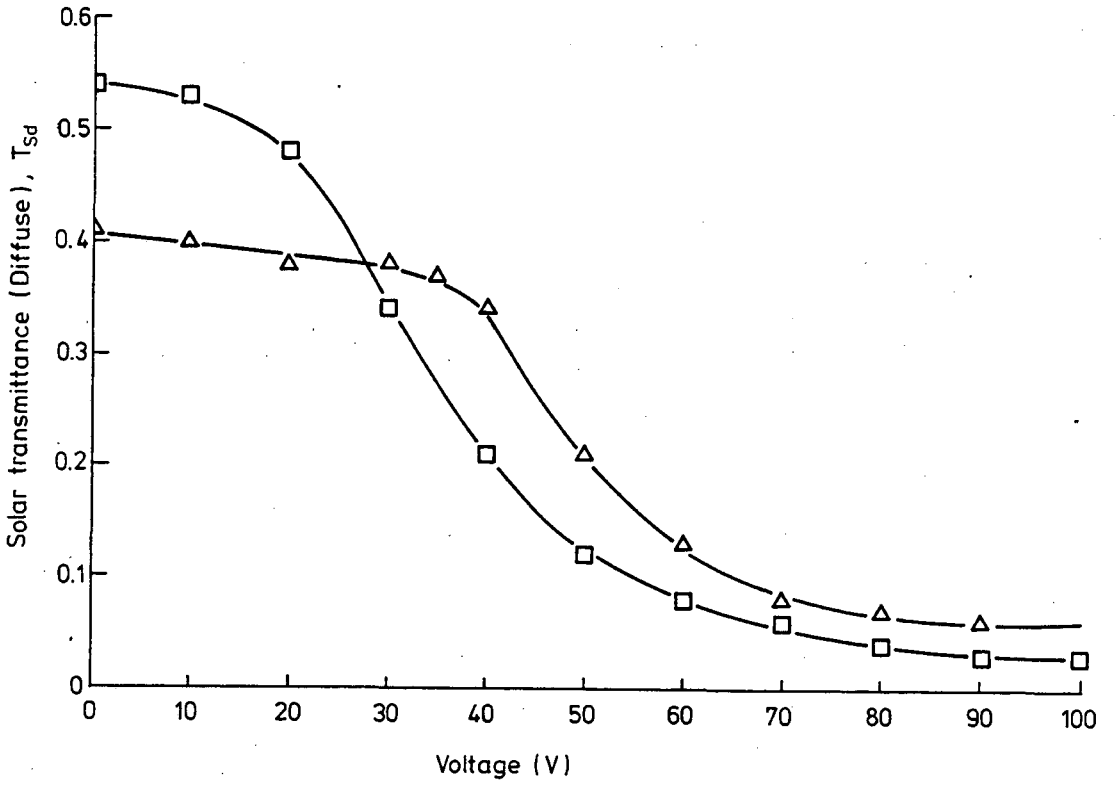

Fig. 7. Comparison of the integrated near-normal hemispherical diffuse solar transmittance values of the dyed (triangle) and undyed (square) Taliq liquid crystal films as a function of applied voltage.

Table 1. Taliq Window Total Transmission Properties

Measurement	Italy	UK	Swit	Germ	Germ (spec)	USA (spec)	Canada
Undyed (305B)							
0V (solar)	0.69	0.64	0.69	0.675		0.043	
100V (solar)	0.73	0.70	0.74	0.731	0.715	0.644 (90V)	
0V (photopic)				0.664		0.01	
100V (photopic)				0.731	0.671	0.669 (90V)	
Undyed (106A)							
0V (solar)	0.73	0.67	0.73	0.717	0.092	0.087	0.158
100V (solar)	0.75	0.74	0.76	0.746	0.671	0.677 (90V)	0.670
0V (photopic)				0.712	0.024	0.03	0.066
100V (photopic)				0.748	0.712	0.690 (90V)	0.624
Dyed (00430)							
0V (solar)		0.44		0.442	0.029		
100 V (solar)		0.71		0.700	0.663		
0V (photopic)				0.200	0.003		
100V (photopic)				0.685	0.639		

Table 2. Taliq Window Diffuse Transmission Properties

Measurement	Swit	UK
Undyed (305B)		
0V (solar)	0.65	0.56
100V (solar)	0.07	0.07
Undyed (106A)		
0V (solar)	0.56	0.54
100V (solar)	0.05	0.03
Dyed (00430)		
0V (solar)		0.41
100V (solar)		0.06
0V (photopic)		0.18
100V (photopic)		0.08

D. References

Bhadur, B., Mol. Cryst. Liq. Cryst. 109(1984)3.

Blinov, L. M. , "Electro-optical and magneto-optical properties of liquid crystals," Wiley, New York, NY (1983).

Busturk, N. and Grupp, J. "Liquid crystal guest-host devices and their use as light shutters," Large-area chromogenics: materials and devices for transmittance control, (Lampert, C. M. and Granqvist, C. G., edits.), Optical Engineering Press- SPIE, Bellingham, WA, (1990)335.

Chandrasekhar, S., Liquid Crystals, Cambridge University Press, Cambridge, England (1977).

de Gennes, P.G., The physics of liquid crystals, Clarendon Press, Oxford, UK (1974).

Drzaic, P. S., "Polymer dispersed nematic liquid crystal for large area displays and light valves" J. Appl. Phys. 60 (1986)2142.

Heilmeier, G. H. and Zanoni, L.A., "Guest-host interactions in nematic liquid crystals-a new electro-optic effect" Appl. Phys. Lett. 13(1968)91.

Fergason, J. L., "Polymer encapsulated nematic liquid crystals for display and light control applications," SID Digest 85(1985)68.

Montgomery, G. P., Jr., "Polymer dispersed and encapsulated liquid crystal films," Large-area chromogenics: materials and devices for transmittance control, (Lampert, C. M. and Granqvist, C. G., edits.) Optical Engineering Press- SPIE, Bellingham, WA, (1990)335.

Sherr, S., Electronic Displays , J. Wiley, NY (1970).

van Konynenburg, P., Marsland, S., and McCoy, S., "Solar radiation control using NCAP liquid crystal technology," Solar Energy Mat. 19(1989)27.

V. DURABILITY TESTING OF LOW-E COATINGS

M. G. Hutchins, U. Frei, V. Wittwer, M. Köhl, V.-V. Truong, T. Hollands, and S. Tanemura

A. Introduction to Low-E Coatings

Transparent low-emissivity (low-E) coatings continue to develop and play a major role in reducing radiative heat transfer in building glazing (Lampert, 1981; Kostlin, 1982; Lampert, 1982; Glaser, 1989). Currently, low-E coatings are used in many double-glazed and multiple-glazed windows. In the near future, a range of spectrally tuned low-E coatings suited in performance, durability, and color for their specific application will be available. It will be interesting to evaluate these spectrally selective coatings when they become products.

Low-E coatings are coatings for glass and plastic that are predominantly transparent over the visible wavelengths (0.3–0.77 μm) or solar wavelengths (0.3–2.5μm) and reflective in the thermal infrared (2.5-100 μm). A selective low-E film will show a strong transmission cut-off at 0.77 μm and a strong reflection cut-on at 0.77 μm. This film is useful for applications where the solar gain from the near infrared is not wanted, e.g., for a large commercial building or automobile. Low-E films for windows derive their usefulness from their low thermal emissivity (or high reflectance) in the infrared. The lower the emissivity, the smaller the magnitude of radiative heat transfer by the window. The hemispherical emissivity of glass is $e_h = 0.84$. Many plastics have high emissivity values, too. A common plastic window film is polyethylene teraphthalate (PET).

Transparent low-E films can be classified into two categories: multilayer dielectric/metal/dielectric (D/M/D or D/M/D/M/D) and highly doped semiconductor. These categories are becoming less defined as semiconductor films are used more in multilayer designs. Multilayer films have an advantage of broad wavelength tunability over the doped semiconductors. Doped semiconductors have the advantage of durability. Properties of commercial low-emissivity coatings are compared in Dolenga (1986) and Bakke (1991). Characteristics are shown for typical commercial window configurations using low-E coatings in Table 1.

The design and theory of D/M/D films are well understood (Eckertova, 1986; Macleod, 1986). Historically, the D/M/D films are not durable enough in window designs to be used on exposed surfaces because of atmospheric corrosion problems. It may be possible, however, to make this class of coating more durable by better material design. Multilayer D/M/D low-E coatings are typically deposited on glass and plastics by physical vapor deposition (PVD), which includes vacuum evaporation and sputtering techniques. The wavelength selective properties of D/M/D films are derived from both the optical properties of the metal and dielectric layers and the interference effects caused by the film stack. Metal films less than approximately 10 nm thick exhibit partial visible and solar transparency. The optical properties of thin metal films have been determined for a range of thicknesses (Karlsson and Ribbing, 1978). The dielectric layers serve both to protect and to partly antireflect the metal film in the visible region, thereby increasing transmission. The dielectric film, usually a metal oxide, when used to overcoat a metal, must exhibit high infrared transmittance in order to preserve the infrared reflectance of the

metal. The metal layer is typically silver, gold, and copper. Silver is used most often. Durability improvement of multilayer films remains an important research area.

Table 1. Characteristics of Glazings Using Commercial Low-E Coatings
(Bakke, 1991)

Type	Shading Coeff.	T_D	U-Value, W/m^{2}K (R-Value)
Double-Pane (for comparison)	0.89	82	2.8 (2)
Low-E, Double Glazed (SnO_2)	0.84–85	74–78	1.72–2.27 (2.5–3.3)
Low-E, Double Glazed (D/M/D, Argon Filled)	0.72	76	1.83 (3.1)
2 Low-E/Plastic, Double Glazed (D/M/D, Argon Filled)	0.52	62	0.71 (8)
Laminated Glass (D/M/D/Plastic)	0.56	74	2.5 (2.2)
Low-E, Triple-Glazed (D/M/D, Argon Filled)	0.61	69	0.84 (6.7)

The most common commercial D/M/D coatings are $In_2O_3/Ag/In_2O_3$, $SnO_2/Ag/SnO_2$, and ZnO/Ag/ZnO. Other coatings of the D/M/D type are $TiO_2/Ag/TiO_2$ and ZnS/Cu/ZnS. Many of these coatings use barrier layers at the Ag/dielectric interface to prevent oxidation of the silver layer during oxide deposition. Typical barrier materials are aluminum oxide, chromium oxide, and lead oxide. Greater selectivity is achieved by making a D/M/D/M/D stack (Woodard and Zeable, 1990). Examples of makers of multilayer coatings are Southwall (Palo Alto, CA) and Renker (Switzerland). The Southwall company received the 1990 product of the year award from Popular Science for its Superglass window. The window uses two low-E suspended polymer films inside a double glazing, with a krypton gas fill. This window has a center-of-glass thermal conductance of U = 0.71 W/m^{2}K (R-8 rating); with the frame, its net U value is probably U = 1.14–1.4 W/m^{2}K (R-4–R-5). Other companies are starting to introduce gas-filled low-E window products, too; these are expected to become a standard in the future. In this study, the properties of multilayer Southwall coatings on PET and Interpane coatings on glass are investigated .

Examples of highly doped semiconductors are SnO_2:F, SnO_2:Sb, In_2O_3:Sn (ITO), Cd_2SnO_4, ZnO:Al and ZnO:In. Doped semiconductor films are typically deposited by chemical vapor deposition (CVD) either on or off the glass float line. This process has been limited to glass and higher temperature materials because of the temperatures involved (400–600 °C). Of the highly doped semiconductors, tin oxide pyrolytic coatings made on the glass float line have been the most successful. In this process, an aqueous tin chloride or tin organometallic liquid with an appropriate dopant or powder is sprayed onto the surface of the glass as it leaves the molten tin float bath. The spray reacts with the hot glass surface (600 °C) in air, forming the tin oxide coating. Problems of iridescence have hampered the use of this glass compared to multilayer coated glass with much more controllable optical properties and lower emissivity. Recently, these tin oxide pyrolytic coatings have been improved by Pilkington (K-Glass) and LOF glass by the use of a two-layer coating to reduce iridescence in thicker tin oxide coatings. This allows a coating with even lower sheet resistance to be produced with excellent optical properties. Also, doped semiconductors can be deposited by PVD, but at lower deposition rates. In our study, pyrolytic low-E coated glass from Ford Glass Company was used. This coating was produced on the glass float line.

B. Measurements

Measurements of normal and hemispherical optical and infrared emittance of three commercial low-E coatings were made. Samples of pyrolytic tin oxide from Ford Glass, and dielectric/metal/dielectric (D/M/D) coatings from Southwall and Interpane were exposed (unprotected) at the Swiss ITR test center. After exposure the optical values were just of the substrate material for the D/M/D coatings. The results showed that the Southwall and Interpane coatings were totally destroyed by exposure and the Ford coating was unchanged. For the D/M/D coating these results were expected because of its inherent fragility. The multilayer coatings are normally used in a protected fashion either inside a window glazing gap or laminated to glass. Further data can be found in the IEA SHC Programme Task 10 Working Documents (Frei and Häuselmann, 1989; and Hutchins, 1990).

1. Instrumentation/Experimental Methods

The UK group determined the optical properties of the low-E coatings by reflectance. The spectral measurements covered the 0.3 to 13 μm wavelength range. An integrating sphere was used for near-normal/hemispherical reflectance and the normal-hemispherical transmittance measurements. In the solar spectral range up to 2.5 μm, a $BaS0_4$-coated integrating sphere has been used. The sphere is attached to a Zeiss PMQ spectrophotometer system. The equipment was calibrated for the solar spectrum (0.3 to 2.5 μm) using $BaS0_4$, for diffuse reflecting samples. The Balzers, Aluflex coating was used a standard for specular reflecting samples. In the infrared, a diffusely reflecting gold integrating sphere was used. This sphere was coupled to a Bruker rapid scan Fourier transform spectrometer. This instrument has enabled us to measure the spectral near-normal/hemispherical reflectance and the normal/hemispherical transmittance in the range from 1.4 to 13 μm. As a standard in the infrared (1.4 to 13 μm), the Labsphere gold coating was used for diffuse reflecting samples. The Balzers, Goldflex coating was used as specular reflecting standard in the infrared. The German group used a Lambda 9 spectrophotometer for their measurements. All measurements were total. The Lambda 9 was

equipped with a Labsphere 150 mm integrating sphere coated with barium sulfate. The detectors were shielded from the ports. A Halon reference standard was used. A light trap was used to exclude background radiation from the sample surface. Finally, the plotted curves were corrected using calibration data from Labsphere. The Canadian group used a Cary 2400 (UV-VIS-NIR) spectrophotometer over 300-2500 nm.

For the integration of solar values, all participants used the (Air Mass 1.5) ASTM E891 or ISO standards. The integrated photopic response was calculated from the standard CIE/ISO photopic spectra. Angular data were also taken on these samples, among others, and can be located in a sister document under an EC project (Hutchins and Ageorges, 1992).

2. Optical Measurements

The integrated transmittance and reflectance data are shown in Table 2 for the three low-E samples. Additional data are written up by the Canadian participants (Truong and Ashrit, 1990). In Table 3 are characteristic spectral data for the Southwall low-E coating (type 2A). The Southwall coating is deposited on PET. All other coatings are on glass substrates. The data in Table 3 are from the German group.

Table 2. Integrated transmittance and reflectance for low-E coatings.

Sample	Property	Solar (AM 1.5)	Photopic
Interpane	T_{dir}	0.537	0.812
	R_{dir}	0.299	0.064
	T_{tot}	0.555	0.820
	T_{dif}	0.037	0.050
	R_{tot}	0.357	0.096
Ford	T_{dir}	0.743	0.824
	R_{dir}	0.121	0.139
	T_{tot}	0.753	0.834
	T_{dif}	0.009	0.011
	R_{tot}	0.152	0.165
Southwall	T_{dir}	0.675	0.856
	R_{dir}	0.378	0.114
	T_{tot}	0.695	0.855
	T_{dif}	0.026	0.032
	R_{tot}	0.273	0.106

Table 3. Spectral data for the Southwall low-E coating (2A)

Wavelength	Transmittance	Wavelength (um)	Transmittance
389.8	77 97	844.8	68.17
446.0	84.08	896.7	64.41
483.3	85.72	979.0	58.26
519.1	86.85	1041.4	53.46
555.4	86.38	1144.4	47.31
592.6	85.27	1253 5	41.14
629.5	83.36	1524.3	32.31
666.7	81.54	1700.1	25.01
707.0	79.46	2322.0	12.08
750.5	75.91		
795.4	72.78		

C. References

Bakke, T. O., "Glass Breakthroughs," Home Mechanix, Feb(1991)55.

Dolenga , J., "Low-E: Piecing together the puzzle," Glass Magazine, March, (1986)116.

Eckertova, L., Physics of Thin Films, 2ed Edit., Plenum, New York, NY, (1986).

Frei, U. and Häuselmann, T. , "Heat Mirror Case Study", IEA Working Document, ITR Phase 1 Report, Rapperswil, Switzerland, (1989).

Glaser, H. J., "Coated heat insulating glass," Glastech. Ber. 62(1989)93.

Haacke, G., "Transparent conducting oxides," Ann. Rev. Mat. Sci. 7(1977)73.

Hutchins, M.G. " Optical properties of transparent Low-emittance coatings" IEA Working Document, Oxford Brookes University, Oxford, UK (1990).

Hutchins, M.G. and Ageorges, P. "Intercomparison of measurements of spectral transmittance and reflectance at different angles of incidence", CBR report, Project 3413/1/0/177/1/91-BCR-UK(30), Oxford Brookes University, Oxford, UK (1992).

Karlsson, B., Ribbing, C. G., UPTEC report, Contract 3879-1, Univ. of Uppsala, Sweden (1978).

Kostlin, H. J., "Application of thin semiconductor and metal films in energy technology," Festkorperprobleme 22 (1982).

MacLeod, H. A., Thin Film Optical Filters, 2nd Edit, MacMillian, New York, NY (1986).

Lampert, C. M., "Heat-mirror coatings for energy conserving windows," Solar Energy Mat. 6(1981)1.

Lampert, C. M., "Materials chemistry and optical properties of transparent conductive thin films for solar energy utilization," Ind. Engin. Chem. Prod. R&D 21(1982)61.

Truong, V-V, and Asrit, P.V., Optical Measurements on the Asahi, Taliq and Low-E coating systems" IEA Task 10C Working Document, University of Moncton, NB, Canada (1990).

Woodard, F. E., Zeable, Z. V., "Optical element for a vehicle windshield" U.S. Patent 4,943,140, Jul. 24 (1990).

VI. INTERLABORATORY TESTING OF TRANSPARENT INSULATION MATERIALS

W. J. Platzer, V. Wittwer, U. Frei, T. Hollands, S. Svendsen, and B. Karlsson.

Below is a general discussion of transparent materials followed by results of interlaboratory tests of some representative materials. The interlaboratory testing not only helped us to measure the optical and thermal properties of these complex materials but also pointed out some measurement technique and instrument differences between the different laboratories.

A. Introduction

Translucent (or transparent) insulation materials (TIM) are materials like solid and granular silica aerogel, low-density glass, and a variety of cellular polymers. The cellular polymers are usually a honeycomb, capillary, or closed-cell construction. Fig. 1 shows generic types of transparent insulation. These polymers are not to be confused with conventional foamed polymers, which are generally considered opaque. Silica aerogel in sheet form does have some unique advantages because it has high clarity in its transmission and does not have highly oriented properties. All other products tend to have strongly oriented structures with a high amount of scattering or diffuse transmittance. These materials can be used in a variety of ways, e.g., as windows, as skylights, as solar collector covers, and as opaque wall insulation.

TIM materials have thermal properties different from those of conventional opaque insulation materials; e.g., the equivalent thermal conductivity (k_e) is dependent on the thickness of the sample. Also, their optical properties are different from those of conventional glazing units. For example, some materials have coarse structures with dimensions of several millimeters. They are up to 15 cm thick, and they can show scattering. Honeycomb structures also split up the incoming beam radiation in a complicated manner. This leads to increased problems of measuring the thermal and optical properties of these materials. Measurement schemes that have been developed for other materials are not necessarily appropriate for transparent insulation materials.

Although there are many different material types, a classification can be given (modified from Platzer, 1988). One may classify the materials according to the nature of the optical path of an incoming beam. Clear glass, for instance, does not distort images on the other side, but diffusing structures do. Also, there are material structures that preserve the incidence angle but still do not allow a clear view. Both criteria are physically meaningful, but there is a continuum of materials between the extreme cases. Mixed types also exist with respect to optical behavior. A honeycomb TIM fabricated from plastic film exhibits both a strong specular component and a weak diffusing component of the transmitted radiation. This is because the plastic film is not completely specular in nature. A classification according to the geometric structure of the materials is very useful. Four generic types are defined as shown in Fig. 1.

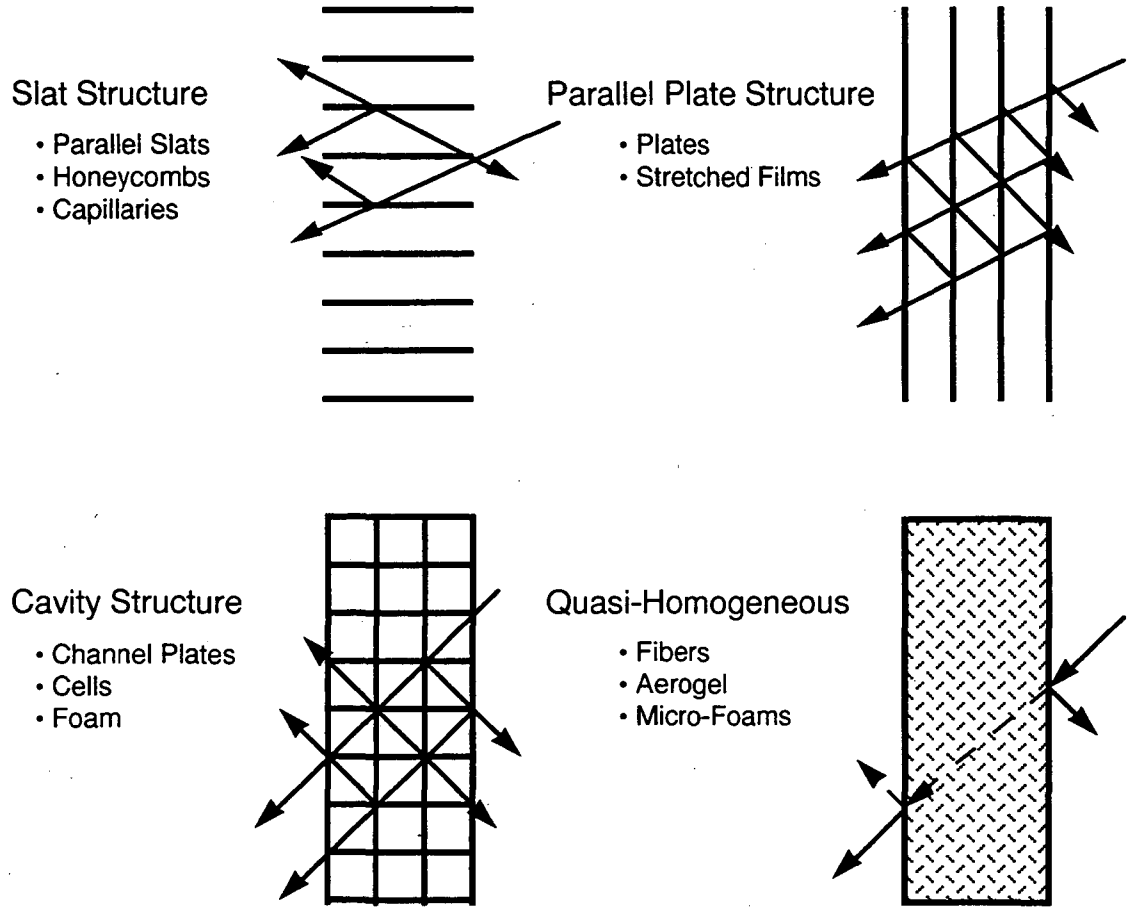

Fig. 1. Four generic types of transparent/translucent insulation structures (XBL 9111-2429). (modified from Platzer, 1988).

One of the best known is the parallel-plate structure with multiple glazings or plastic films, which may be either transparent or translucent. The specular multiple-glazed window even fits in this category (although it is not considered translucent insulation). The Geilinger (Winterthur, Switzerland) super window is an example. High optical reflection losses prohibit the use of a large number of layers. The glass panes or plastic films have defined temperatures (approximately constant), but because of convection in the gaps between, a one-dimensional temperature distribution cannot be given.

The slat structures include honeycomb or capillary materials with different cross-sectional geometry and slit structures (plastic films stretched parallel across the glazing). As the incoming beam is reflected and transmitted by the structure walls toward the absorber, optical losses are very small. Only some scattering and absorption within the films reduce the overall transmittance. For clear films with low absorption, the transmission properties are nearly independent of the material thickness; therefore very thick samples may be used. Contrary to the first type, the parallel-plate structures, convection can be suppressed if the proper aspect ratio is chosen.

If the previous types are combined, one gets a cavity structure, represented by transparent multiple duct plates or transparent foam with bubble sizes on the order of millimeters. From an optical viewpoint, these materials have approximately the same transmittance as an equivalent multiple-film cover. Reflection is the dominant loss mode. The materials have the advantage, however, of being even more effective in suppressing convection losses, but conduction paths are longer than they are in the first two structure types.

Quasi-homogeneous layers are characterized by similar optical properties, but the loss mechanisms are scattering and absorption. Aerogel, a microporous silica foam, belongs to this class. Because the pore sizes are some 10 nm, light is scattered within the material, comparable to the Rayleigh scattering of blue sky. This structure is very effective in the reduction of convective loss. Glass fiber materials do not have this homogeneity, but they can be treated and analyzed with similar methods.

For each of the four generic types, theoretical approaches exist that satisfactorily describe the basic features of the materials. Of course, transition materials exist that cannot be strictly classified. Folded or V-corrugated films are one example. If the corrugation angle is small, the glazing behaves essentially like a parallel-plate material; if the angle is large, it behaves nearly like a slat structure. Honeycomb structures with cells not vertically oriented with respect to the glazing plane are a transition between the parallel-plate and the cavity structure types. Nevertheless, the generic types provide a useful approach to classification of these materials. The energy modeling and optical characterization of these materials still require considerable work. It is expected that in the future more of these materials will be used in the development of super glazings. An evaluation has been made of several transparent insulation materials for building facades (Van Dijk et al., 1990; Wittwer and Platzer, 1990) .

B. Aerogel

One of the major drawbacks of conventional windows is their high thermal loss characteristics compared to other building walls. Transparent low-emissivity surface treatments and modified window design can help lower the radiative portion of heat transfer. A way of decreasing conductivity is to reduce overall conduction through the glazing. A complimentary approach is to develop a highly transparent material that by virtue of its bulk macro- or microstructural properties has low thermal conductivity. Aerogel is such a material. Its properties have been investigated and reviewed by several authors (Rubin and Lampert, 1984; Mazur and Lampert, 1984; Fricke, 1986; Russo and Hunt, 1986; Henning, 1990). The commercial manufacturers of monolithic aerogel are Airglass (Lund, Sweden) and Aerojet (Sacramento, CA). The commercial cost of producing monolithic aerogel was estimated to be as little as 20 US$/m^2 (Kahn, 1991). Aerogel panels made by Airglass were studied. Granular aerogel is made by BASF in Germany and Monsanto in the U.S. Other types of aerogels exist; recently the first organic aerogel was made at the Lawrence Livermore Laboratories (Livermore, CA) consisting of carbon, hydrogen, and oxygen.

Monolithic silica aerogel is very close to being a specular transmitting insulating material. Aerogel has a microstructure of bonded fine silica particles surrounded by porous microcells. The pore size is approximately 10 nm. Only 2-5% of the volume is solid silicon dioxide; the 95-

98% remainder is filled with air. The thermal conductivity of aerogel is lower than still air because the microcells are smaller than the mean-free-path of an air molecule (about 66 nm). Since most of the particles are smaller than a wavelength of visible light, they are not strongly scattering in the visible. But the size and distribution of the micropore structure can account for scattering of visible light, resulting in a small amount of haze. However, haze can be effectively reduced by process control. Aerogel has optical properties similar to silica glass except that the index of refraction (n = 1.03-1.1) is much lower than glass. This material has been optically modeled using Rayleigh Theory. Silica aerogel is made by producing a colloidal silica gel from hydrolysis and polycondensation reaction of an orthosilicate. This gel is solidified into the form of its mold by CO_2 substitution for the alcohol solvent, followed by supercritical drying. This chemical process was developed by (Tewari, 1985; Russo and Hunt, 1986). The advantage of the CO_2 substitution process is that much lower temperatures and pressures can be used to form the aerogel making it a safer, more economical, and faster process. The disadvantage of aerogel is that it must be protected from shock and moisture. It is possible to form aerogel between two sheets of glass to make a window. The volumetric density of aerogel is around 135 kg/m^3.

For a window of aerogel (20 mm thick), the thermal conductance (U) is calculated (Rubin and Lampert, 1984) to be about 1 W/m^{2}K (or thermal resistance of R = 5.7 h-ft^2/Btu^{o}F). For a double glazing without aerogel (20 mm spacing), U = 2.8 W/m^{2}K (R = 2.0 h-ft^2/Btu^{o}F). The solar hemispherical transmission properties for aerogel are better than T_S = 0.67 (20 mm thick) and T_S = 0.9 (5 mm thick). A very low thermal conductance of U = 0.5 W/m^{2}K (R = 11.4 h-ft^2/Btu^{o}F) can be achieved for a double glazing by evacuating the aerogel to about 0.1 atm. (Büttner et al., 1984; Hartmann, Rubin and Arasteh, 1987). An evacuated monolithic aerogel window of 0.57 m x 0.57 m x 0.2 m has been constructed at the Thermal Insulation Laboratory in Denmark (Jensen, 1990). The optical properties of aerogel windows have solar transmittance values for diffuse irradiation of about 0.4 to 0.7, including the necessary cover glazings (e.g., aerogel granules usually are filled into a double glazing unit) while having heat loss coefficients U (or k) between 0.7 W/m^{2}K and 2.0 W/m^{2}K.

C. Polymers

A range of polymeric materials with macrostructures containing open or closed cells and oriented micro-channels have been experimented on as transparent insulation (Platzer, 1987; Pflüger, 1987). There is considerable European interest in the development of translucent insulation as thermal insulation for windows and walls. Although these materials generally provide a non-spectular view for window applications they can be used for building insulation or skylights. Also, these materials can be used for the insulation of solar collector covers and thermal storage tanks. Many types of TIM polymer microstructures exist, ranging from capillaries to honeycombs to cavity structures. These materials are typically composed of polycarbonates and acrylic polymers. U values of 0.8 W/m^2 have been achieved with solar diffuse transmission values of greater then 70%. (Wittwer and Platzer, 1990). The morphological effects on the transparency of these materials have been studied (Alexander-Katz, 1990). Measurement techniques for these optically complex materials are being developed at the Fraunhofer-Institute for Solar Energy Systems, Freiburg, FRG. (Platzer, Apian-Bennewitz and Wittwer, 1990).

Polymeric transparent insulation materials combine high solar transmittance with good heat insulation properties when compared to conventional single or double glazings. Some polymeric materials are available as commercial products, e.g., Arel (Israel) polycarbonate capillary structure (measured in this study) and Okalux (Germany) cell structures. The materials available have solar transmittance values for diffuse irradiation of about 0.4 to 0.7 including necessary cover glazings, U value (k value) of 0.7 W/m^2K and 2.0 W/m^2K. The Arel polycarbonate honeycomb structure has cell widths of about 4.5 mm, cell walls between 20 and 100 microns (mean thickness of 55 microns), and a volumetric density of approximately 36 kg/m^3. The structure is produced from extruded multi-ribbon strips (width equivalent covering 4 rectangular cells) glued together.

D. Interlaboratory Testing

Transparent insulation materials have thermal properties different from conventional opaque insulation materials, e.g., the (equivalent) thermal conductivity (k_{eq}) is dependent on the thickness of the sample. Also optical properties are different from conventional glazing units, e.g., some materials have coarse structures with dimensions of several millimeters. They may be as thick as 15 cm and they usually show scattering. Honeycomb structures split up the incoming beam radiation in a complicated manner. This leads to increased measurement problems. Measurement schemes developed for other materials may not be appropriate for transparent insulation materials.

To investigate problems associated with measurements, an interlaboratory comparison of two types of materials was performed. The Arel polycarbonate honeycomb, and Airglass monolithic aerogel were chosen as samples. The types of measurement performed on these samples were determined by available equipment in each participant's laboratory. Only two participants (Sweden, Germany) had large integrating spheres to determine the angular dependent solar transmittance. The Dutch group (NL) built an integrating sphere and made measurements on the Airglass sample during the latter stage of the study. The UK laboratory used a simple technique consisting of a solar cell detector panel, which gave approximate results.

Identical samples were sent out by the companies Arel and Airglass to the participants. The companies sent out samples from the same production run to each participant. The required measurement properties were the heat conductance, k [W/m^2K], and the angular-dependent direct-diffuse solar transmittance, $T_S(A)$. The Airglass slab of aerogel had a thickness of 12-13 mm. To protect the fragile structure, it was glazed on both sides with conventional float glass making a total thickness of 20 mm. However, the glazing broke during transport to the German team. The glass was replaced by one with low iron content. The original and replacement glass were measured in a spectrophotometer to account for the difference between the glasses. For the interlaboratory test, Arel sample thicknesses of 5 cm and 10 cm were evaluated. The samples were not covered with any glazing, but every participant was told to protect the samples from dust.

1. Thermal Conductance of Polymer Honeycomb and Aerogels

1.1 Description of Apparatus

The thermal conductance of TIM samples were measured in a hot-plate apparatus. Each sample was pressed tightly between two high-emissivity endplates. This ensures that no air flow between different cells of the honeycombs could occur. In the measurement, the sample is covered with side insulation of at least 5 cm Styrofoam (or equivalent) and on the inner side with low-emissive aluminum foil. Using this procedure minimizes the edge effects of thermal conduction and radiation, which otherwise would disturb the one-dimensional net heat transport within the samples. The aluminum foil is necessary in contrast to conventional measurements. Because the Arel aerogel material is partially transparent to infrared radiation, a cold side insulation would act as a heat sink and a hot side wall (when compared to the material temperature) would act as a heat source.

Heat conductance was measured at 20°C, 40°C, and 60°C mean temperature of the material with approximately 15–20 K temperature difference between the plates. As convection should not occur within the narrow honeycomb cells at these temperatures (but not for the aerogel), according to previous measurements of the Freiburg group, the tilt of the experimental setup was regarded as not important. As for the materials considered and for the setup with plates tightly pressed to the materials, no large reduction in heat conductance should occur for low-emissive endplates. Some laboratories did additional experiments to confirm those findings. low-emissive end-plates were used by Denmark, Canada, and Germany. The latter two laboratories also tested the variation of heat transport with tilt angle, which would change if convection were present. The heat loss coefficient measurements were taken at room temperature with slight variations. For transparent insulation materials used in solar collectors, higher temperatures would have to be used. Hot-plate devices using heat flux meters have to be calibrated for the whole temperature

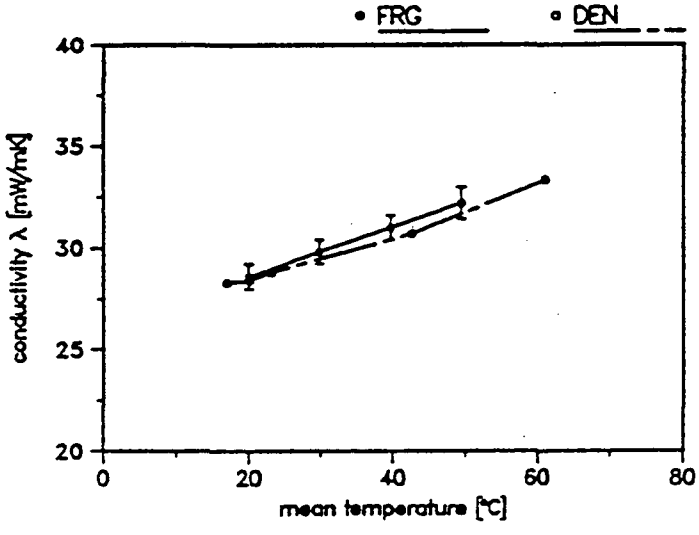

Fig. 2. Comparison of temperature-dependence of heat flux meter calibration using measurements on opaque standard Styrofoam material (2 cm thickness) performed in the Swedish and German laboratories.

range, as heat flux meters show a explicit temperature dependence of their sensitivity. A check of the temperature dependent calibration between two laboratories is shown in Fig. 2. The good agreement shows that the calibration is identical within the error bounds for these laboratories. comparison of a measurement standard would give even more confidence in the devices. However, it was agreed this should be done only when large discrepancies between the results of different laboratories show up. Every laboratory has its own set of calibration checks and some laboratories use an absolute method for calibration.

1.2 Measurements

The heat conductance for three samples over a range of temperatures were measured by various laboratories. The data is shown in Figs. 3-6. Although the accuracy is not very great, as is expected for a 'standard measurement', the shape of the lines are in agreement. One has to note that these materials are not standard insulation materials, and therefore, have different behavior from normal materials. The most important difference is that they are partially transparent to infrared radiation. Therefore, the end plate emissivities play an important role for heat transport within the honeycomb structures, but nearly none for the aerogel, which is nearly opaque in the infrared. The aerogel slab was not heat treated before the measurements. If the sample was annealed, the conductivity would be influenced by lowering the water content. Also, the sample was not evacuated between the two glass panes. Evacuation leads to an even smaller conductivity as shown by Büttner, et.al. The influence of end plate emissivities is shown in Fig 6. Because the honeycomb structure is semitransparent to infrared radiation, one low-emissive end plate (10% emissivity) and a high-emissive one (case SB) give about 20% lower results than two high-emissive end plates (case BB).

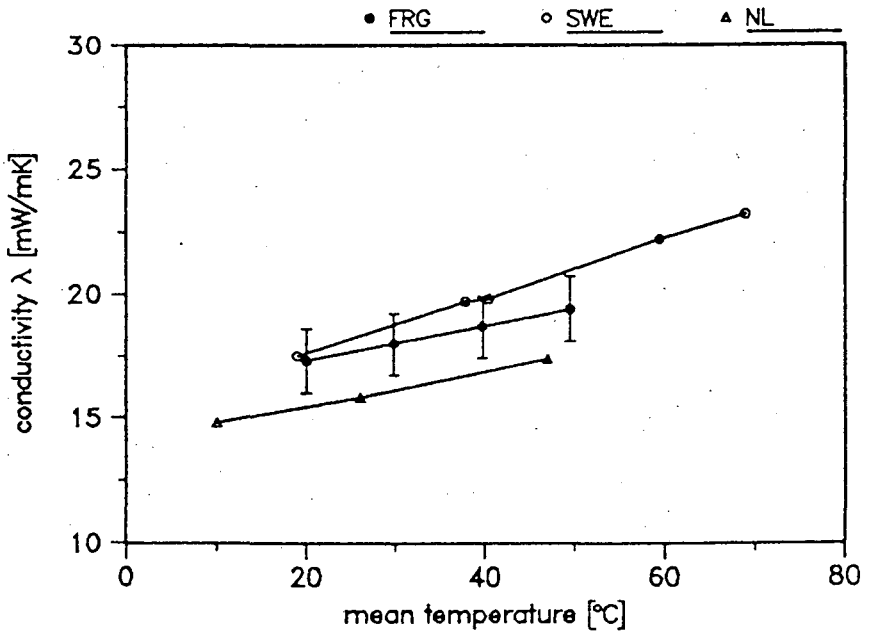

Fig. 3. Heat conductance for an airglass aerogel window unit (with aerogel thickness of 13 cm and 20 mm total thickness with glass). The heat resistance of the coverglasses is neglected, so the conductivity of the unit is attributed only to the aerogel.

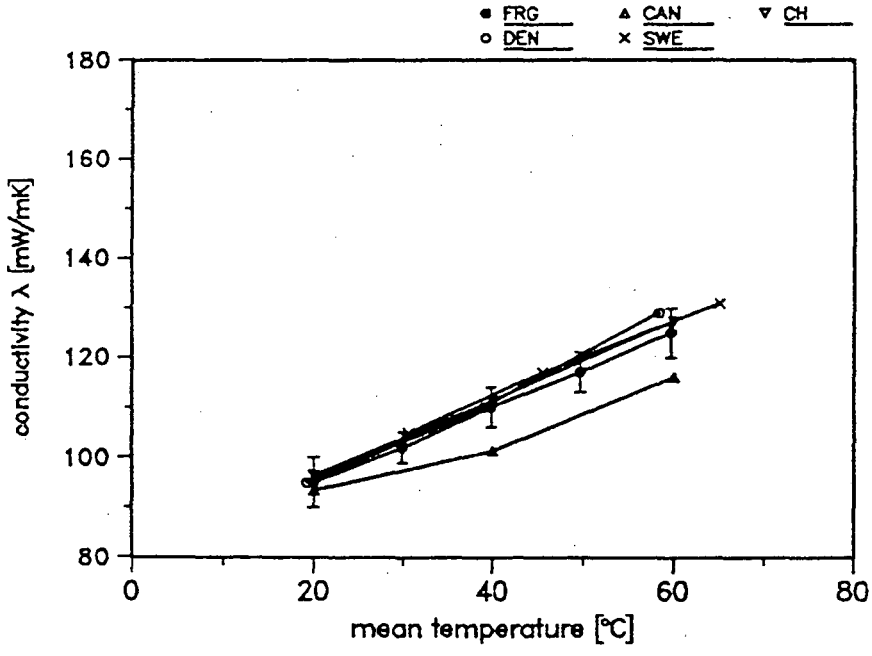

Fig. 4. Heat conductance for an Arel polycarbonate honeycomb sheet with thickness of 5 cm.

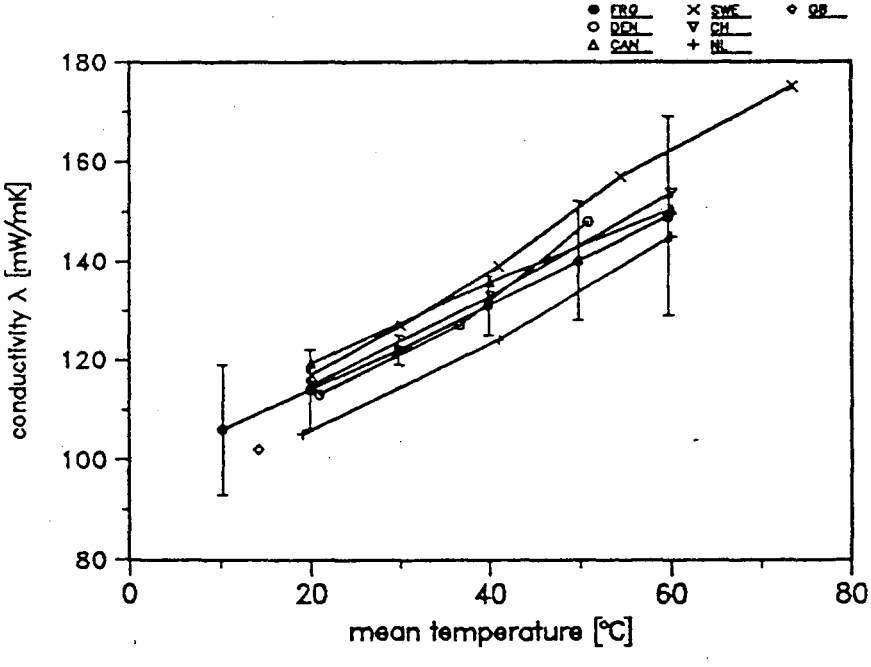

Fig. 5. Heat conductance for an Arel polycarbonate honeycomb sheet with thickness of 10 cm.

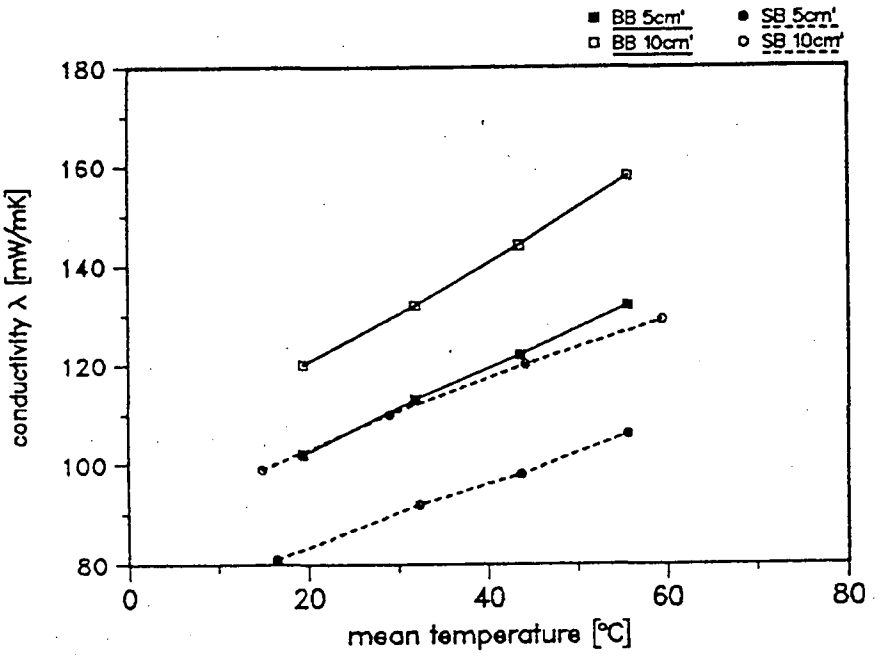

Fig. 6. Heat transport through a polycarbonate honeycomb sheet (10 cm), showing dependence on end-plate emissivities.

All results (except the UK result) were determined in the horizontal position of the sample. Convection should be suppressed for high aspect ratio honeycomb cells and low Rayleigh numbers. This was also confirmed by results from the German group, where the inclination of the heat flux apparatus with sample did not change the heat flux significantly (within limit of accuracy).

The large thickness of the honeycomb samples and their partial transmission to infrared radiation makes it necessary to well insulate the edges of the samples against ambient temperature and include an infrared reflector foil at the edges. A perfectly reflecting foil would simulate an "infinite sample size" to infrared radiation, reducing the effect of the edge. Aluminum foil has very good reflection properties in the infrared and was found to reduce the errors due to edge effects. The heat conductance values for a 10 cm Arel honeycomb material with and without the reflector foil at the edges are shown in Fig. 7. The curve without a reflector foil overestimates the heat fluxes for high temperatures, as the edge losses due to radiation transport are increasing.

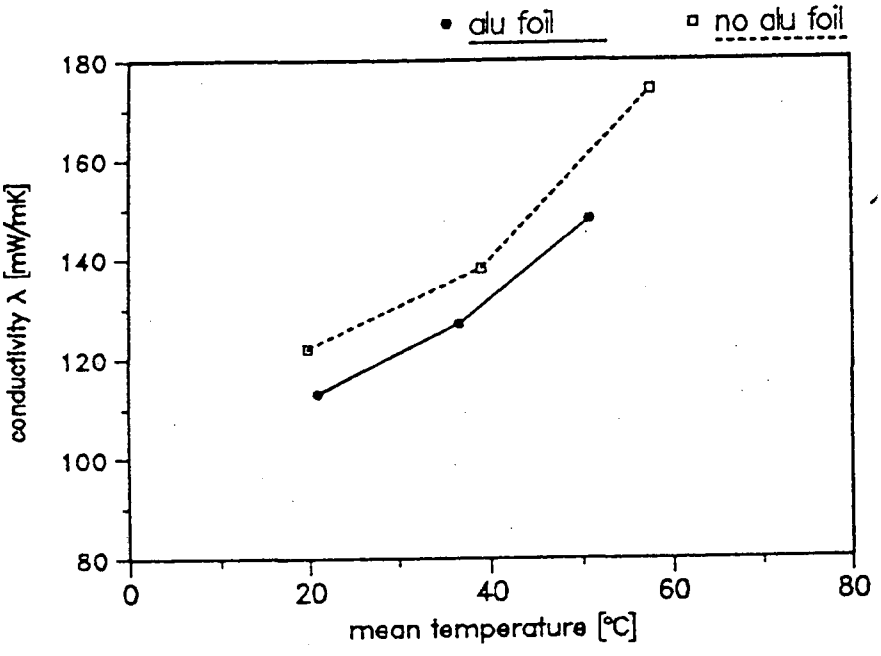

Fig. 7. Heat transport characteristics through a 10 cm thick Arel honeycomb sample. The difference between measurement with and without aluminum foil at the edges is shown.

2. Angle-dependent Solar Transmittance of Polymer Honeycomb and Aerogels:

2.1 Description of Apparatus

The experimental setup should ensure that a representative average solar transmittance of the samples could be measured without large effects of the coarse structure of the samples (honeycombs) and without large errors due to edge effects because of the sample thicknesses (up to 10 cm). Therefore, the radiation beam and detector diameter should be much larger than a single honeycomb cell diameter, and the side part of the thick honeycomb samples should be covered with highly reflecting foil (aluminum or silver). This simulates a good approximation of an 'infinite sample' by a mirror effect.

The two available integrating spheres were both relatively large allowing a sufficiently large area of the sample to be illuminated. A simple technique was used by one laboratory (UK). It used a solar cell panel placed behind the sample as a detector and a solar simulator. This approach, is limited since the spectral sensitivity of the solar cells is quite pronounced. This is especially important for aerogel. Another preliminary trial using a pyranometer and natural sunlight was not successful. One problem was the small detection area of the pyranometer. A second problem was the requirement that the detector should collect radiation from all solid angles of the hemisphere transmitted by the sample. Unfortunately, the detector area cannot be placed close enough to the back surface of the illuminated sample because of the domed pyranometer glass

cover. This may become important for large incidence angles. The third practical problem with this method was that natural light from the direct sun served as the illumination source. Obviously, the diffuse background from the sky poses the most severe problem concerning the data interpretation. But the fluctuations in time may be difficult to handle. As a consequence of these problems, the results contained some error.

2.2 Measurements

Figs. 8-10 show the measurement results for the three different samples, measured by the three participating groups (SWE, FRG, UK). They show the directional-hemispherical (or direct-diffuse) transmittance dependent on incidence angle. Whereas the calculation of a diffuse-diffuse transmittance for isotropic sky radiation may be easily calculated from these curves for the case of aerogel, as this is an material with rotational symmetry, it poses some problem for the honeycomb structures. Here a complete characterization certainly needs a specification of the polar and the azimuthal incidence angle, hence a larger number of scans with the materials rotated would be needed in these cases. However, in non-perfect structures (having corrugated walls and scattering in the cell walls) the incident ray reorients within the structure, and the influence of the azimuthal incidence angle may be neglected (Platzer, Apian-Bennewitz, and Wittwer , 1990). Therefore, the numbers for the diffuse-diffuse transmittance ($T_{s,dif}$) have been calculated from the single curves shown in the figures. The measured values have been linearly extrapolated up to a 90 degree incidence angle.

The large transmittance values for high incidence angles measured by the UK group (designated GB) are probably not a consequence of the spectral selectivity of the detector, but come from edge illumination of the thick samples. This error could be minimized by covering the edges with reflecting films. Edge sealing has been necessary for the German group sphere set-up (FRG), where the whole sample is illuminated. But for the Swedish measurements, a small diameter beam is used and this does not illuminate the edge. For the Swedish set-up the range of incidence angles is only limited by the beam to sample geometry.

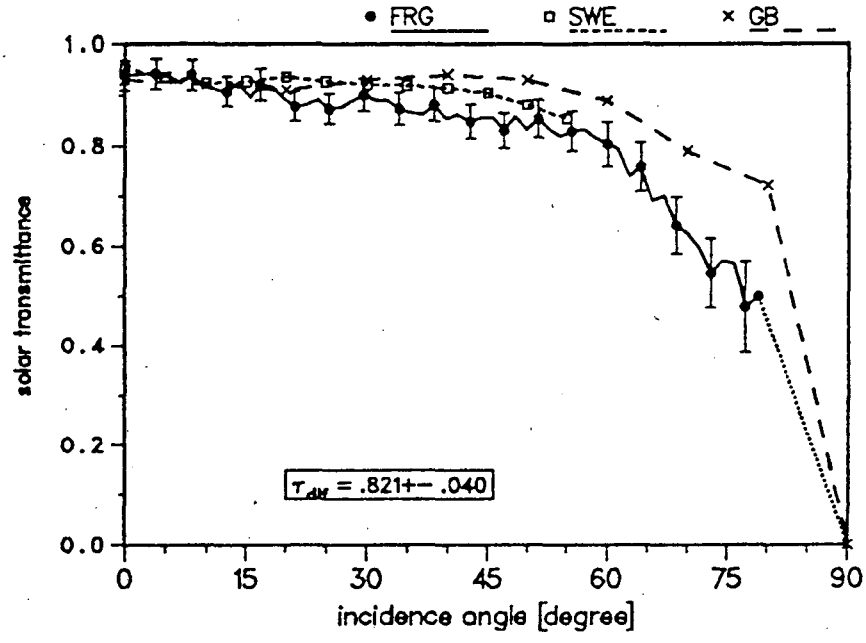

Fig. 8. Solar transmittance $T_S(A)$ verses incidence angle for a 5 cm Arel polycarbonate honeycomb sheet.

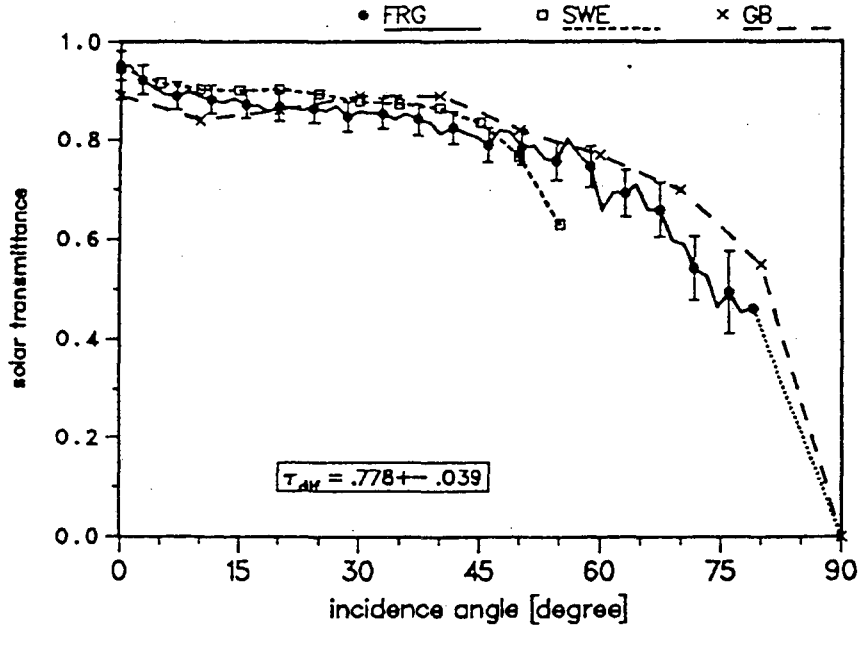

Fig. 9 Solar transmittance $T_S(A)$ verses incidence angle for a 10 cm Arel polycarbonate honeycomb sheet (sample A).

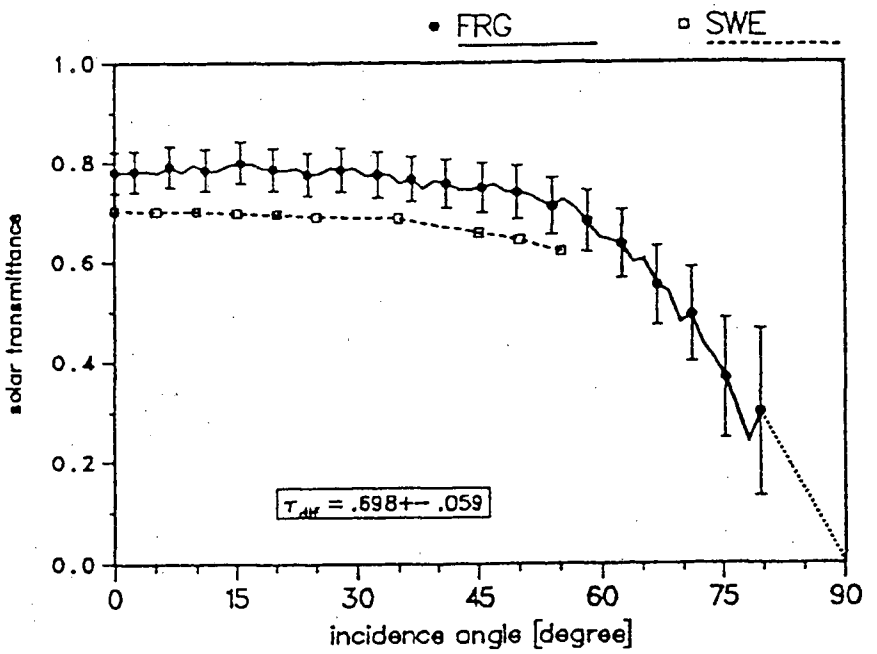

Fig. 10. Solar transmittance $T_S(A)$ verses incidence angle for a 1.3 cm thick Airglass aerogel sample between two glasses. SWE used two sheets of 4 mm float glass, and FRG used two sheets of 3 mm low-iron glass.

For the Airglass sample the original glazing was broken during the transport to Freiburg/FRG. Therefore, a different glass cover was used to protect the sample. The replacement glass cover has a solar transmittance close to 92% for vertical incidence, which was slightly different from the original glazing. The effect of the different glazings was corrected with a simple model for the triple layer glass/aerogel/glass. The absorption coefficient of the original glazing was determined using the solar transmittance for a AM 1.5 spectrum calculated from spectrometer transmission data ($T_{S(AM\ 1.5)}$=0.86). The corrected data are shown in Fig. 11.

The results for aerogel show that the spectral sensitivity of the solar cell detector is important for this type of material. The detector has its maximum sensitivity at approximately 1100 nm, but there the scattering of the aerogel, which is strongly wavelength dependent, is relatively small when compared to the blue part of the spectrum. Therefore, the solar transmittance is overestimated.

The Swedish laboratory measured the transmittance of the aerogel slab and the glazing unit composed of glass sheets and aerogel. Fig. 12 gives a comparison of the pure slab and the three-layer glazing unit.

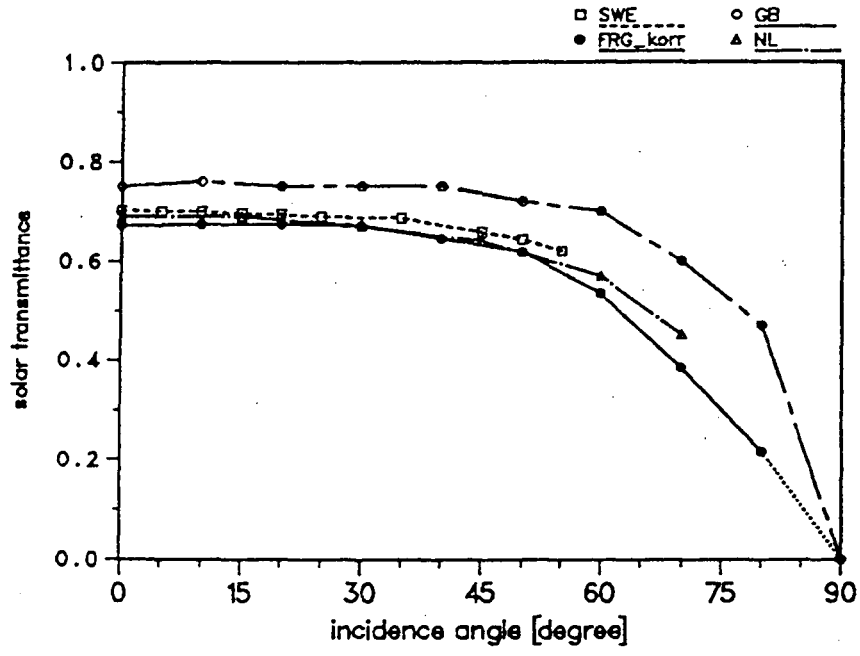

Fig. 11. Solar transmittance verses incidence angle for a 1.3 cm thick aerogel sample between two glass sheets (The FRG curve is corrected for the original float glass).

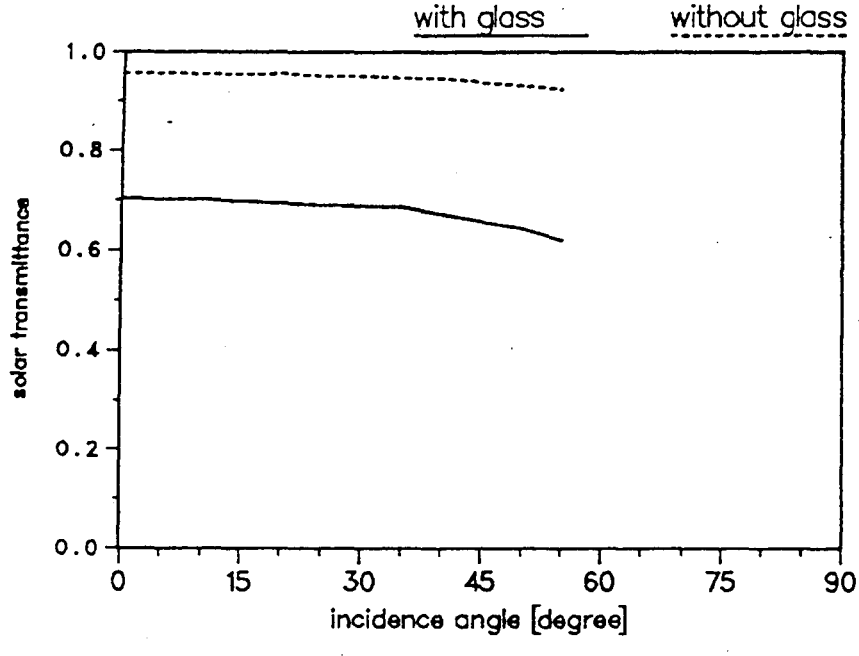

Fig. 12. Comparison of angular solar transmittance for monolithic aerogel and aerogel on a glazed unit.

3. Summary of Thermal and Optical Measurements

The following tables give thermal conductance and solar transmittance results for the three samples. The first number gives the U-value linearly extrapolated to 10 C average temperature of the sample, including the internal and external surface coefficients, respectively, h_i = 8 W/m^{2}K and h_{ext} = 23 W/m^{2}K. Values with other coefficients may be calculated accordingly. The second value gives the solar transmittance for vertical (normal) incidence; the third number, the solar transmittance for isotropically diffuse solar transmittance (if calculated by the participant). The complete results are compiled in a working document (Platzer, 1990).

Thermal conductance and solar transmittance for the 5 cm Arel polycarbonate honeycomb sheet:

	U-Value [W/m^{2}K]	$T_{s,n}$	$T_{s,dif}$
Canada	1.38	-	-
Denmark	1.77	-	-
Germany	1.36	0.94	0.84
Netherlands	-	-	-
Sweden	1.38	0.95	-
Switzerland	1.68	-	-
UK	-	0.93	-

Thermal conductance and solar transmittance for the 10 cm Arel polycarbonate honeycomb sheet:

	U-Value [W/m^{2}K]	$T_{s,n}$	$T_{s,dif}$
Canada	0.94	-	-
Denmark	0.88	0.85-0.95	0.75
Germany	0.91	0.95	0.78
Netherlands	0.86	-	-
Sweden	0.91	0.93	-
Switzerland	0.90	-	-
UK	0.90	0.90	-

Thermal conductance and solar transmittance for the Airglass aerogel sample:

	U-Value [W/m^{2}K]	$T_{s,n}$	$T_{s,dif}$
Canada	-	-	-
Denmark	-	0.61	0.53
Germany	1.07	0.68	0.60
Netherlands	0.99	0.69	-
Sweden	1.05	0.70	-
Switzerland	-	-	-
UK	-	0.75	-

E. Conclusions

Through testing, we obtained the following results for the Arel honeycomb (5 cm): $T_{s,normal}$ = 0.93–0.95, $T_{s,diffuse}$ = 0.84, U = 1.38–1.77 W/m^{2}K. For the 10-cm honeycomb, we found the following:$T_{s,normal}$ = 0.85–0.95, $T_{s,diffuse}$ = 0.75–78, U = 0.88–0.94 W/m^{2}K. For the aerogel, we measured $T_{s,normal}$ = 0.61–0.75, $T_{s,diffuse}$ = 0.53–0.60, and U = 0.99–1.07 W/m^{2}K. The range in values indicated the variation in measurements from different laboratorys. From this work, we found that some of the thermal test equipment gave significantly different results from laboratory to laboratory. We uncovered some common measurement problems, such as edge conduction along highly insulating windows (e.g., aerogels). Overall, this study helped some of the participants to make better thermal measurements.

The interlaboratory comparison of transparent insulation materials was a very useful activity since it uncovered some common measurement problems of these materials. The activity was not of sufficient scope, however, to exactly determine the source of measurement errors for each participant. Also, the accuracy was limited by the fact that the samples were only similar, not equal. A round-robin testing of a single sample would have avoided that problem, but because of the fragile character of the samples, it was decided not to do this. Another method that would help make results more comparable would be to use a lead laboratory, which would be responsible for sending out precharacterized samples. The samples could also be tested at the same laboratory after they have been circulated to the other laboratories. This approach again has some transportation problems. A lead laboratory with enough manpower was needed, and the time schedule would have been extended. Also, the results showed that accuracy in the measurement of transparent insulation materials is not high enough to justify a more ambitious testing scheme.

F. References

Alexander-Katz, R., "The morphological effects on the transparency of optically inhomogeneous composites," Proc. SPIE 1272(1990)309.

Büttner, D. et. al.,"Thermal conductivity of evacuated highly transparent aerogel", Report E12-0784-1, Phys. Inst. Univ. Würzburg, Würzburg, Germany (1984).

Fricke, J. edit., Aerogels, Springer-Verlag, Berlin, Germany (1986).

Hartmann, J., Rubin, M., and Aresteh, D., "Thermal and solar-optical properties of silica aerogel for use in insulated windows," Proc. of 12th Annual Passive Solar Conf., Portland, OR, July 12-16, (1987).

Henning, S., "Airglass-Silica aerogel, a transparent heat insulator," Report D7:1990, Swedish Council for Build. Res., Stockholm, Sweden (1990).

Jensen, K. I., "Transparent cover with evacuated monolithic silica aerogel," Proc. Northsun Conf, (1990).

Kahn, J., "Lightweight aerogels can make a solid contribution to energy conservation," LBL Res. Rev. 16 (1991)3.

Mazur, J. H. and Lampert, C. M., "High resolution electron microscopy study of silica aerogel transparent insulation," Proc. SPIE 502(1984)123.

Pflüger, A., "Minimum thermal conductivity of transparent insulation," Solar Energy Mat. 16(1987)255.

Platzer, W. J. "Solar Transmission of Transparent Insulation Materials", Sol. Energy Mat., Vol. 16, pp. 275-287 (1987).

Platzer, W. J., "Solare Transmission und Wärmetransportmechanismen bei transparenten Wärmedämmaterialien," Doctoral Thesis, Albert-Ludwigs-Univ., Freiburg (1988).

Platzer, W. J., Apian-Bennewitz, P., and Wittwer, V., "Measurement of hemispherical transmittance of structured materials like transparent insulation materials," Proc. SPIE 1272 (1990)297.

Platzer, W. J., "Interlaboratory testing transparent insulation materials," IEA Task 10/C Report, Sept. (1990).

Rubin, M. and Lampert, C. M., "Transparent insulating silica aerogels," Solar Energy Mat. 11(1984)1.

Russo, R. E., and Hunt, A. J., "Comparison of ethyl versus methyl solgels for silica aerogel using polar nephelometry," J. Non Cryst. Solids 86(1986)219.

Tewari, P. H., Hunt, A. J., and Lofftus, K. D., "Ambient temperature supercritical drying of transparent silica aerogel," Materials Lett. 3 (1985) 363.

Van Dijk, H. A. L., Van Paassen, J. P., Van der Stel, R. and Arkesteijn, C. A., "Translucent thermal insulation in facades. An investigation" (In Dutch) Physische Dienst TNO-TH, Delft, Netherlands, TNO-TPD-814.017, TNO-TPD-914.070, NOVEM-90-318 Feb. (1990).

Wittwer, V. and Platzer, W., "Transparent insulation materials," Proc. SPIE 1272(1990)284.

VI. OVERALL CONCLUSIONS FOR SUBTASK C

Several characterization parameters were developed for electrochromics. Optical properties, electrical properties, and efficiency measurements were studied. Under optical properties, the properties of solar and photopic transmittance, reflectance, and absorptance; optical density; and chromaticity coordinates were analyzed and discussed. For electrical measurements, injected charge, impedance, potential type, voltammetry, switching chronopotentiometry, point-of-zero-zeta-potential, and cycle energy and power were studied. Under efficiency and response measurements, coloration efficiency, response time, and memory were detailed. The most poorly defined parameters were injected charge, coloration efficiency, response time, and memory. Our work helped to define these better and to point out some of the related issues.

Field testing of the Asahi electrochromic window demonstrated that even a fairly absorptive window can have significant control over energy flow through a window. In the MoWiTT field tests, an approximate 30% reduction in heat flow with a constant interior illumination level was achieved compared to a static bronze glazing. Integrated visible transmittance changed from 0.78 to 0.20 when a voltage of –2.0 V was applied across the device. The transmittance–voltage dependency was determined for these devices, memory and coloration rate were measured and the chromaticity coordinates determined. This device did not have good memory, however, so power needed to be applied continuously. Other electrochromic devices have been shown to have better memory properties. This technology is very promising for the next generation of windows. The interaction of performance and cost needs to be studied further.

Phase dispersed liquid crystal optical switching devices (PDLC) were provided by Taliq Corporation for testing. The typical undyed PDLC device has very broad switching, but its net change in hemispherical transmittance is only about 25% over the solar and visible spectrum when 100 V ac is applied. A similar device using dyed liquid crystals showed much improved visible control of 50% change. These devices appear to have the best use for privacy and skylight applications. The biggest issues are cost and UV durability.

The optical properties of low-E coatings were confirmed in this study. Samples were supplied by several manufacturers: pyrolytic tin oxide from Ford Glass, dielectric/metal/dielectric (D/M/D) coatings from Southwall on plastic, and from Interpane on glass. The coatings were exposed outdoors (unprotected) at the Swiss ITR test center. The D/M/D coatings were totally destroyed by exposure, and the pyrolytic coating was unchanged. For these silver-based D/M/D coatings, these results were expected because of their inherent fragility. This confirmed that the D/M/D coatings can not be exposed to normal weathering without protective coatings, and that tin oxide coatings are potentially durable enough to be used in exposed applications.

Two types of commercially interesting transparent insulating materials (TIM) and glazings were studied. Measurements involved thermal testing and angular and hemispherical optical property testing. Honeycomb polycarbonate made by Arel, Israel, and aerogel made by Airglass, Sweden, were tested in a round-robin test procedure. There was some variation in the thermal results due to differences in equipment and procedure indicating that further refinements in these procedures or facilities is needed.

In total, this subtask provided useful results to the researchers involved and resulted in the creation of Task 18, Advanced Glazing Materials, to extend many of topics initially explored in Task 10. The most significant part of this work is probably the fact that people from several countries were brought together to compare the results from their differing equipment on standard samples. There were differences in both measurement equipment and procedures. This subtask helped standardize measurements of advanced and fairly complex glazing, compared to conventional glass. The work helped verify the accuracy of different types of equipment. It indicated which equipment was best for particular measurements or sample types. In some cases the results pointed out the pitfalls of certain measurements and allowed each laboratory to determine if it needed to upgrade or modify its equipment or change a measurement procedure. This was especially apparent with the interlaboratory comparison of properties of transparent insulation materials, since it uncovered some common measurement problems with these materials. The TIM results showed the measurement of transparent insulation materials does require better techniques to provide accurate thermal measurements, which are now being addressed in Task 18.

In the longer term, results of this work should lead to more standardized measurements and progress toward more uniform international standards related to glazing materials. In round-robin testing, a single sample was best, but transportation of the sample around the world was a problem because of the fragile nature of glass. A preferred method of distribution is to have several samples that are premeasured by a lead laboratory and then sent out. Upon return, they could be measured again at the lead laboratory. The multiple sample distribution technique is recommended for future tasks. The subtask developed new procedures and methods to test new glazings, such as the electrochromic glazing, that have never been tested before. Many participants in the group had limited or no experience with several of the materials studied in the subtask but were experienced with standard glazings.

The participation of companies such as Taliq, Asahi, Arel, and Airglass in supplying prototype and commercial samples for this activity helped considerably. The work gave these companies data from new measurements and confirmed industry measurements on their materials. Furthermore, the outcome of the materials measurements generated valuable thermal and optical data that is essential for energy modeling. Participating researchers valued the opportunity to share tests and results with international collaborators. For example, it would be highly unlikely that the electrochromics groups of Asahi Glass, LBL, Oxford Brooks University, and the Fraunhofer Institute would ever form a joint project without this IEA SHC task. Subtask C made it possible to obtain samples of prototype electrochromic and liquid crystal glazing. Participants learned about specialized equipment that would be useful for future measurements. Several informal collaborations and information networks were formed as a direct result of the subtask activities.

INTERNATIONAL ENERGY AGENCY

The International Energy Agency, headquartered in Paris, was founded in November 1974 as an autonomous body within the framework of the Organization for Economic Cooperation and Development (OECD) to coordinate the energy policies of its members. The twenty-three member countries seek to create the conditions in which the energy sectors of their economies can make the fullest possible contribution to sustainable economic development and the well-being of their people and the environment.

The policy goals of the IEA include diversity, efficiency and flexibility within the energy sector, the ability to respond promptly and flexibly to energy emergencies, the environmentally sustainable provision and use of energy, more environmentally-acceptable energy sources, improved energy efficiency, research, development and market deployment of new and improved energy technologies, and cooperation among all energy market participants.

These goals are addressed in part through a program of collaboration in the research, development and demonstration of new energy technologies consisting of about 40 Implementing Agreements. The IEA's R&D activities are headed by the Committee on Energy Research and Technology (CERT) which is supported by a small Secretariat staff in Paris. In addition, four Working Parties (in Conservation, Fossil Fuels, Renewable Energy and Fusion) are charged with monitoring the various collaborative agreements, identifying new areas for cooperation and advising the CERT on policy matters.

IEA SOLAR HEATING AND COOLING PROGRAM

The Solar Heating and Cooling Program was one of the first collaborative R&D agreements to be established within the IEA, and, since 1977, its Participants have been conducting a variety of joint projects in active solar, passive solar and photovoltaic technologies, primarily for building applications. The twenty members are:

Australia	France	Spain
Austria	Germany	Sweden
Belgium	Italy	Switzerland
Canada	Japan	Turkey
Denmark	Netherlands	United Kingdom
European Commission	New Zealand	United States
Finland	Norway	

A total of nineteen projects or "Tasks" have been undertaken since the beginning of the Solar Heating and Cooling Program. The overall program is monitored by an Executive Committee consisting of one representative from each of the member countries. The leadership and management of the individual Tasks are the responsibility of Operating Agents. These Tasks and their respective Operating Agents are:

*Task 1: Investigation of the Performance of Solar Heating and Cooling Systems - Denmark
*Task 2: Coordination of Research and Development on Solar Heating and Cooling - Japan
*Task 3: Performance Testing of Solar Collectors - Germany/United Kingdom
*Task 4: Development of an Insulation Handbook and Instrument Package - United States
*Task 5: Use of Existing Meteorological Information for Solar Energy Application - Sweden
*Task 6: Solar Systems Using Evacuated Collectors - United States
*Task 7: Central Solar Heating Plants with Seasonal Storage - Sweden
*Task 8: Passive and Hybrid Solar Low Energy Buildings - United States
*Task 9: Solar Radiation and Pyranometry Studies - Canada/Germany
*Task 10: Material Research and Testing - Japan
*Task 11: Passive and Hybrid Solar Commercial Buildings - Switzerland
Task 12: Building Energy Analysis and Design Tools for Solar Applications - United States
Task 13: Advanced Solar Low Energy Buildings - Norway
Task 14: Advanced Active Solar Systems - Canada
Task 15: Not initiated
Task 16: Photovoltaics in Buildings - Germany
Task 17: Measuring and Modeling Spectral Radiation - Germany
Task 18: Advanced Glazing Materials - United Kingdom
Task 19: Solar Air Systems - Switzerland
Task 20: Solar Energy in Building Renovation - Sweden
*Completed

LAWRENCE BERKELEY LABORATORY
UNIVERSITY OF CALIFORNIA
TECHNICAL INFORMATION DEPARTMENT
BERKELEY, CALIFORNIA 94720